Landsc Ecol (2023) 38:821–845
https://doi.org/10.1007/s10980-023-01595-0

RESEARCH ARTICLE

Prediction-based approach for quantifying phenological mismatch across landscapes under climate change

Yiluan Song · Stephan B. Munch · Kai Zhu

Received: 24 October 2022 / Accepted: 9 January 2023 / Published online: 27 January 2023

Abstract

Context Climate change is driving phenological shifts across landscapes, but uncoordinated shifts might cause a potential "phenological mismatch." There has been little consensus on the existence and magnitude of such a mismatch. The lack of agreement among studies can be attributed to the wide variety of definitions for the term "phenological mismatch," as well as the methods used to measure it. The lack of comparability among measures of phenological mismatch creates a challenge for conservation.

Objectives We proposed a novel theoretical framework to generalize existing measures of phenological mismatch and an approach to quantify the decoupling between phenology and the environment using the loss in predictive skill over time. We aimed to estimate the magnitude of phenological mismatch on large spatial scales and test the proposed predictive approach's ability to detect multiple types of phenological mismatch.

Methods We modeled historical climate-phenology coupling and quantified phenological mismatch as the deviation between observed and predicted phenology under climate change. First, we used two large empirical spatiotemporal datasets to estimate phenological mismatch in plant flowering phenology in the eastern United States and bird reproductive phenology in Finland. Historical climate-phenology coupling was modeled with spatial linear regression. Second, we conducted four simulation experiments representing different types of mismatch during climate change. We recovered simulated phenological mismatch by fitting a data-driven nonlinear model (Gaussian Process Empirical Dynamic Modeling) and predicting phenology.

Results In the eastern US, we found that advancing plant flowering phenology generally matched spring warming from 1895 to 2015, with seven out of the 19 species studied having significant phenological mismatches, with observed flowering time earlier than predictions even considering warming. A similar phenological mismatch was found in birds in Finland from 1975 to 2017, with the bird breeding season advancing more than expected in 21 out of the 36 species studied. In four simulation experiments, we were able to accurately recover the simulated phenological mismatches in the timing of events, pace

Supplementary Information The online version contains supplementary material available at https://doi.org/10.1007/s10980-023-01595-0.

Y. Song · K. Zhu
Department of Environmental Studies, University of California, Santa Cruz, CA, USA

S. B. Munch
Department of Applied Mathematics, University of California, Santa Cruz, CA, USA

K. Zhu (✉)
Institute for Global Change Biology and School for Environment and Sustainability, University of Michigan, Ann Arbor, MI, USA
e-mail: zhukai@umich.edu

of development, and intensity of activities, although with greater challenges in quantifying a mismatch in life history.

Conclusions Overall, these case studies show that our prediction-based measure effectively quantifies multiple types of phenological mismatch, providing a more generalizable and comparable measure of phenological mismatch across study systems and scales. This study will enable the investigation of phenological mismatch at large scales, improving understanding of the patterns and consequences of climate-change-induced phenological changes.

Keywords Anthropocene · Asynchrony · Climate change · Empirical dynamic modeling · Phenology · Synchrony

Introduction

Since Cushing (1969) proposed the match-mismatch hypothesis, ecologists have been increasingly concerned with whether climate change induces a "phenological mismatch." Phenological mismatch can lead to negative ecological consequences on multiple scales of ecology: from species interactions (Rafferty et al. 2015; Renner and Zohner 2018) to the persistence of populations (Nicola et al. 2011; Visser et al. 2012), and ecosystem functioning (Beard et al. 2019). Meta-analysis shows that the relative timing of key life cycle events in aquatic and terrestrial ecosystems in 1951–2013 has changed significantly since the early 1980s (Kharouba et al. 2018). For example, advancing spring conditions have driven cascading trophic mismatch in the food web from vegetation, insects, birds, to polar bears in the Arctic (Rockwell et al. 2011; Reneerkens et al. 2016). Understanding and mitigating phenological mismatch become particularly crucial given the rapid climate change and human modifications of the landscapes.

Phenological mismatches have been observed either between species and climate or between interacting species. On the one hand, phenological shifts do not always change in concordance with climate change. In a global meta-analysis (Parmesan and Yohe 2003), while 423 out of 484 species changed in their phenology as predicted given the climate change, 61 changed opposite to the prediction. Some phenological mismatches may be the results of anthropogenic activities. For example, in the Midwest US, although warming spring temperatures potentially allowed earlier crop emergence, the remotely-sensed start of season was delayed, due to the replacement of wheat and oat by corn and soybean (Zhang et al. 2019). On the other hand, the widespread phenological mismatch between interacting species under climate change received more attention. For example, the temporal shift in the arriving and hatching of several migratory bird species have been insufficient to match the rapid advancement of spring greenup at their destinations (Visser et al. 1998; Both and Visser 2001; Gaston et al. 2009; Clausen and Clausen 2013; Mayor et al. 2017).

Although phenological mismatch is well studied, our understanding of its magnitude, impacts, and how it changes across scales remains limited. For example, there have been inconsistent findings on whether there are community-level phenological mismatches (Edwards and Richardson 2004; Donnelly et al. 2011; Burthe et al. 2012; Ovaskainen et al. 2013). Part of these inconsistencies arises from the different definitions and methods used to quantify phenological mismatch. Ecologists have realized the difficulty to define a baseline for "matching phenology" (Kharouba and Wolkovich 2020), particularly under global change, as we do not always know how much a species should be shifting to match the change in its environment (Visser and Both 2005). In addition, recent development in phenological mismatch on the community level (Edwards and Richardson 2004; Renner and Zohner 2018) and from a spatial perspective (Post et al. 2008; Vitasse et al. 2018; Aikens et al. 2020) have highlighted the need to expand the concept of phenological mismatch, which traditionally focuses on the population level and a single site. The lack of a coherent and generalizable theoretical framework creates a challenge for understanding and interpreting phenological mismatch across landscapes under climate change.

In this study, we first review the different measures used to quantify phenological mismatch, classifying them into a descriptive approach and a model-comparison approach. After reviewing their advantages and drawbacks, we propose a novel theoretical framework to define a generalized phenological mismatch and measure it with a predictive approach. Last, we conduct three case studies with empirical and simulated data to demonstrate the power and limits of our

new predictive approach in detecting and quantifying phenological mismatch.

Measures of phenological mismatch

The earliest and most common approach to evaluating phenological mismatch is timing-based, i.e., focusing on the relative timing of phenological events (Fig. 1a). One example is the difference in the timing of phytoplankton blooms and fish breeding (Cushing 1969). The main assumption is that there is an optimal time lag between a pair of phenological events (Satterthwaite et al. 2014), and deviations from this time lag indicate a phenological mismatch. These measures can be further divided into two subcategories. Most studies that use a timing-based approach focus on discrete phenological events, such as peak abundance (Blondel et al. 1993; Reed et al. 2013; Doiron et al. 2015) or emergence (Tikkanen and Julkunen-Tiitto 2003; Satterthwaite et al. 2014) (Fig. 1a[1]). Timing-based approaches are often used on the phenologies of species with trophic interactions. In Kudo and Ida (2013), phenological mismatch was measured by the delay in initial bee activity from flowering onset. Reed et al. (2013) defined the phenological mismatch as the difference between the laying date of the first clutch of great tits and the date of peak food abundance, plus 30 days, where both positive or negative mismatch leads to lower

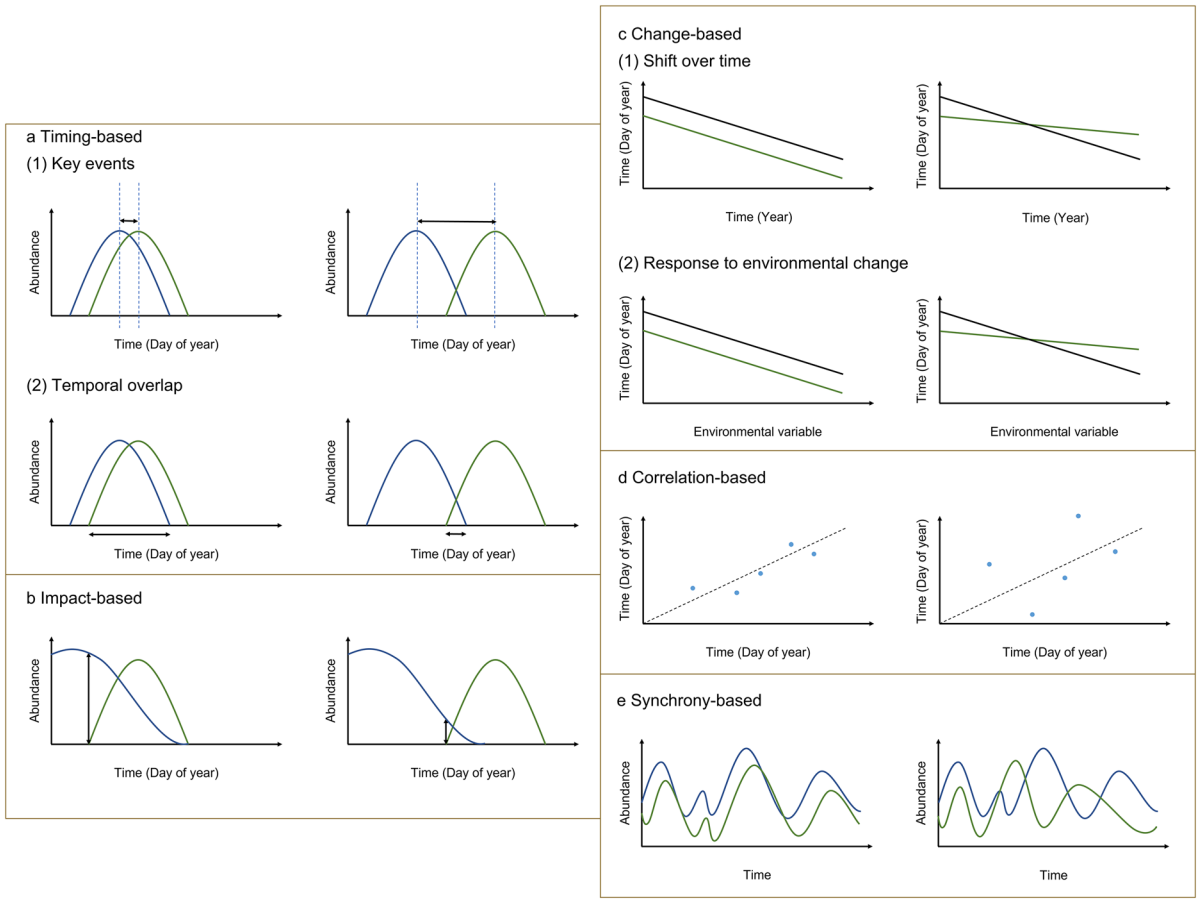

Fig. 1 Conceptual diagrams of five main methods of measuring phenological mismatch. **a** Timing-based methods focus on the relative timing of phenological events or periods. **b** Impact-based methods focus on the consequences of changes in the relative timing of a focal species and its environment. **c** Change-based methods focus on the change of phenological events over time or in response to environmental change. **d** Correlation-based methods focus on the strength of linear coupling between variables. **e** Synchrony-based methods focus on the coordination among processes

fitness. Other timing-based studies treat phenology as a continuous event, such as the continued presence of a species or an environmental condition, and calculate the overlap in timing (McKinnon et al. 2012; Iler et al. 2013) (Fig. 1a[2]). Estimation of timing-based mismatch usually requires knowledge of the time lag or overlap that optimizes fitness or population size (Durant et al. 2005). Such knowledge may be gained from empirical data (Reed et al. 2013; Plard et al. 2014; Satterthwaite et al. 2014; Doiron et al. 2015) or models (Jonzén Tikkanen and Julkunen-Tiitto 2003; Niclas et al. 2007). However, more often, there is no visible ecological consequence of varying time lag (Pearce-Higgins et al. 2010; Dunn et al. 2011; Dunn and Møller 2014), and assumptions are used based on expert knowledge.

Impact-based methods focus on the consequences of changes in the relative timing of a focal species and its environment (Fig. 1b). The consequences may be on the state of resource availability, environmental conditions, or other variables that affect fitness. A classic example is the quantification of mismatch between the coat color change of snow hares and the presence of snow (Zimova et al. 2014, 2016). The researchers defined a hare to be mismatched when the contrast between its coat color and background exceeded 60%. Another index based on impact is "thermal delay," which measures the increase in accumulated degree-days when migratory birds arrive at their breeding grounds (Saino Nicola et al. 2011). The abundance (Durant et al. 2005; Hipfner 2008; Burger et al. 2012) or diversity (Post and Forchhammer 2008; Post et al. 2008) of a group of prey in predator(s)' diet has been used as a proxy for temporal overlap. Similarly, Rafferty and Ives (2011) and Petanidou et al. (2014) measured the level of pollination during flowering. The impact-based measures are closely linked to ecological consequences. Nevertheless, similar to timing-based measures, sufficient knowledge has to be obtained to determine the optimal state of environmental conditions for the focal species.

Change-based methods de-emphasize the relative timing and instead focuses on its change (Fig. 1c). Unlike the previous timing-based method that can be used to evaluate phenological mismatch given a pair of timing in a single year and site based on optimal relative timing, the change-based methods detect changes in relative timing with multiple pairs of timing observed over space or time. This approach has been increasingly popular in recent years because of rapid global change and widespread phenological shifts. One method is to compare the rate of change in the timing of phenological events over time, where a non-parallel shift is considered to indicate a mismatch (Fig. 1c[1]). This method has been used to suggest several mismatches between the reproductive phenology of animals (often birds and ungulates) and environmental cues such as climatic events (Van Noordwijk et al. 1995; Sanz et al. 2003; Gaston et al. 2009; Jones and Cresswell 2010; Clausen and Clausen 2013) and peak food abundance (Visser et al. 1998; Gaston et al. 2009; Plard et al. 2014). The mismatch is less supported in some tightly coupled relationships, such as between flowering and pollinator activities (Bartomeus et al. 2011; McKinney et al. 2012). Notably, this method allows the comparison of more than two species on the community level. Meta-analyses involving multiple taxa suggested differential phenological change among trophic levels (Edwards and Richardson 2004; Both et al. 2009; Thackeray et al. 2010; Burthe et al. 2012; Ovaskainen et al. 2013). The other change-based method is to compare the response in the timing of phenological events to an environmental change, i.e., comparing the sensitivity or slope of the regression line (Fig. 1c[2]). Species that change their phenology differently compared to their interacting species in response to environmental change are considered to face the risk of mismatch (Evans et al. 2013). Observations are often made in experimental settings (Liu et al. 2011; Paull and Johnson 2014) or along environmental gradients (Mjaaseth et al. 2005; Forrest and Thomson 2011; Evans et al. 2013; Iler et al. 2013). Change-based methods have been argued to provide an unbiased measure because it considers species that show little phenological change, which may be under-reported otherwise (Thackeray et al. 2010). However, the result may be sensitive to the time period and area studied. It should also be noted that historical starting points may not benchmark matching phenology due to maladaptation (Blondel et al. 1993) or anthropogenic impacts.

Correlation-based methods are occasionally used, examining the strength of the coupling between the timing of a pair of phenological events or between phenology and environmental conditions (Fig. 1d), with a high correlation coefficient representing a greater degree of "matching." By comparing the

timing of shrimp hatching and spring phytoplankton bloom at various latitudes, Koeller et al. (2009) concluded that the shrimp hatching phenology generally matches food availability in the North Atlantic basin. Bloom timing of plankton has been correlated with sea bottom temperature (Koeller et al. 2009) and ice-retreat timing (Ji et al. 2013). In a North Sea pelagic food web, the lack of significant correlations among species phenologies and with sea surface temperature were used as evidence of a trophic mismatch (Burthe et al. 2012). This method requires the assumption of a relatively tight linear coupling between variables.

Very few studies use synchrony-based methods, examining the synchrony of time series of biotic or abiotic variables (Fig. 1e). Synchrony usually refers to coordination among processes (Ravignani 2017). Although synchrony can be tested statistically (e.g., with time-lagged correlation), visual inspection is employed more often in practice, limited by the amount of data. For example, the life cycles of fast-growing spring plankton advanced synchronously following earlier spring climatic events, whereas slow-growing summer zooplankton displayed no such synchrony, suggesting a higher risk of phenological mismatch (Adrian et al. 2006). The synchrony between the hatching curves of a pest and the bud burst curve of birch was disrupted in cold years but maintained in warmer years (Jepsen et al. 2011). Synchrony-based methods do not require identifying key phenological events but flexibly consider the continuous changes in processes (Yang and Rudolf 2010). They are also less dependent on knowledge of the underlying mechanism, compared to the other methods, because much information can be learned through past temporal dynamics (Nakazawa and Doi 2012). However, whether asynchrony is indeed an accurate reflection of phenological mismatch deserves further research, as asynchrony may reflect adaptive strategies (Visser et al. 2012) and represent a stable state in the absence of climate change (Singer and Parmesan 2010).

We broadly classified the five methods into two main approaches (Fig. 2). The first approach focuses on describing key characteristics of phenological time series (timing of key events, temporal overlap, and impact at a specific time) and comparing the descriptive measure to an optimal measure informed by ecological knowledge (Fig. 1a, b). The second approach focuses on fitting models to phenological metrics and compares model parameters (Fig. 1c, d, e). In the change-based method, linear models are fitted for the relationship between phenological metrics and time (year) or environmental variables, and the slopes are compared. In the correlation-based method, the error of models is compared. In the synchrony-based method, the phases of wave functions are compared. The common idea of methods with the model comparison is that matching phenology is represented by some optimal model parameters.

These two approaches have their limitations. For the descriptive approach, the key descriptive measure cannot always be specified, especially for activities with weak or irregular seasonality (e.g., tropical forest phenology) (Wu et al. 2017). The optimal descriptive measure that represents matching phenology requires accurate ecological knowledge, which is not always available. For the model-comparison approach, the models used for phenological metrics are often over-simplistic (usually linear) (Keenan et al. 2020) and lack flexibility.

Crucially, using different methods to study the same system can lead to divergent conclusions. For example, despite the differential response of flowering and syrphid phenology, environmental changes resulted in more days of temporal overlap between the flower-syrphid community through early snow melt (Iler et al. 2013). Different interpretations may even arise from similar methods and results, as there is often no clear distinction between "match" and "mismatch," such as when the shifts in phenology are only partially consistent in a complex community (Burthe et al. 2012; Ovaskainen et al. 2013). Such mixed messages on phenological mismatch arise from the different definitions of phenological mismatch, from the divergence in the research protocol, and from the intrinsic complexity of the climate-phenology system. We argue that a new approach is needed in defining and measuring phenological mismatch that is compatible with the diverse phenological response to climate change and can be similarly applied to all levels of the organization.

A new framework based on prediction

We first seek to define a generalizable baseline for "matching phenology" with minimal assumptions

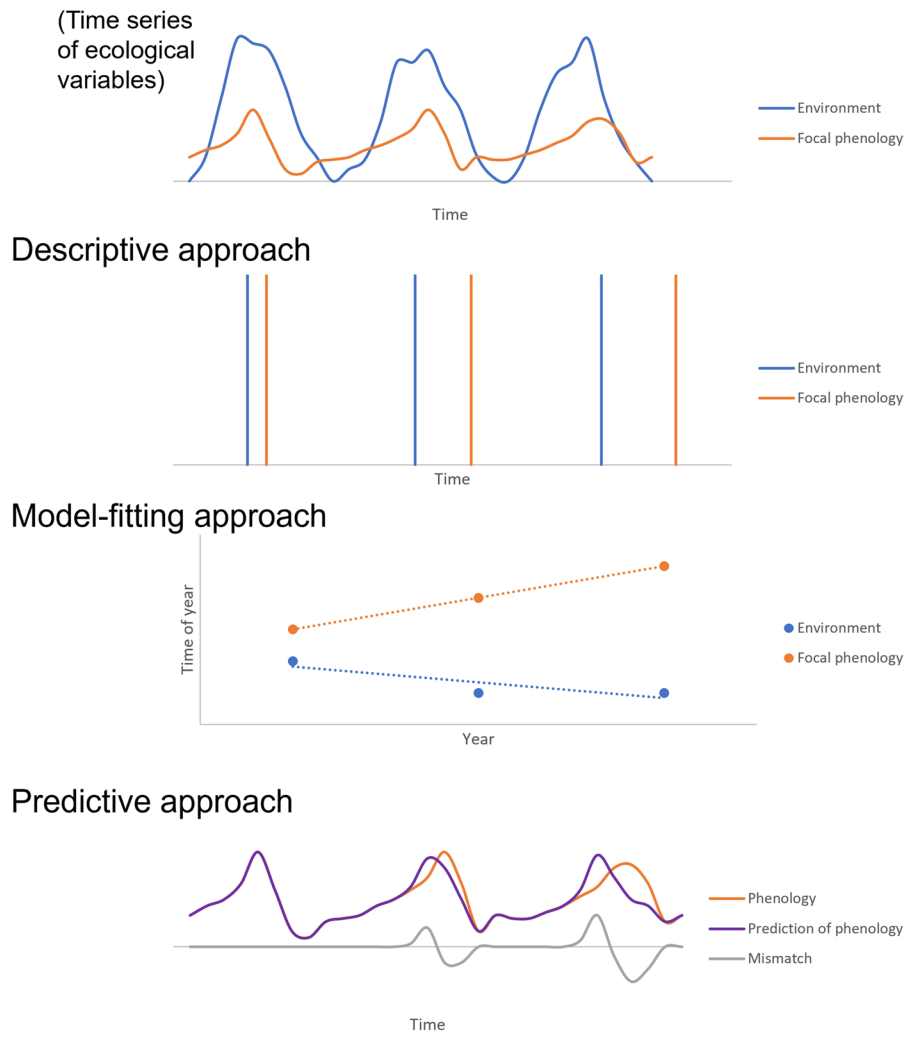

Fig. 2 Conceptual diagram of two existing approaches (descriptive and model-comparison) approach and our proposed approach (predictive) for quantifying phenological mismatch using time series of ecological variables

on the key feature of phenological time series and the structure of phenology models. To generalize the commonly-used definitions, we consider phenological mismatch to take place when the temporal dynamics of individuals, populations, species, components of the ecosystem, or patches in a landscape do not maintain a stable relationship during climate change. Motivated by complex systems theory, we consider phenological mismatch to be the consequence of a loss of "generalized synchronization" (GS), which describes if a (static) functional relation exists between the states of the systems of interest (Kocarev and Parlitz 1995; Rulkov et al. 1995; Abarbanel et al. 1996; Brown and Kocarev 2000; Boccaletti et al. 2002).

Definition Generalized synchronization in the phenology-environment coupling system occurs when there is a function, Φ, such that.

$$Y_{s,t} = \Phi(\boldsymbol{X}_{s,t}) \tag{1}$$

where Φ is a nonlinear function describing the relationships between focal phenology (Y) and the environment ($\boldsymbol{X}$), including the phenology of interacting individuals/populations/communities and abiotic conditions. All variables are indexed by space (s) and time (t), which encourages an explicit definition of the spatiotemporal scale of the synchronization. The same functional relationship (Φ) may be found to be consistent on one scale but not another. For example, the relationship may be consistent within a spatial

range of d (the distance between s_1 and s_2) or only at the same location ($d=0$). The indices are omitted from here onwards for simplicity.

This definition then leads to a natural method for quantifying phenological mismatch, i.e., predicting phenology assuming a static relationship with other phenological and environmental variables, and assessing the discrepancies from observed phenology. This notion of quantifying the extent of GS based on the predictability of time series has been applied in previous studies of simulated chaotic systems and neuroscience (Schiff et al. 1996; Wiesenfeldt et al. 2001). A loss of GS can be detected from a loss in the predictive power of the model (Fig. 2).

The evaluation of phenological change and mismatch starts with a baseline of phenology (Y) and phenology-environment coupling (Φ) (Fig. 3).

$$Y = \Phi(\boldsymbol{X}) \tag{2}$$

If Φ remains the same with changes in the environment ($\boldsymbol{X}_{new}$), we consider there to be no phenological mismatch. This can be expressed as

$$Y_{pot} = \Phi\left(\boldsymbol{X}_{new}\right) = \Phi(\boldsymbol{X}) + \left[\Phi\left(\boldsymbol{X}_{new}\right) - \Phi(\boldsymbol{X})\right] = Y + \Delta Y_{pot} \tag{3}$$

where we refer to the model-predicted phenology given $\boldsymbol{X}_{new}$ as the potential phenology (Y_{pot}), and its difference from Y as potential phenological change (ΔY_{pot}), reflecting the ideal adaptation in focal phenology without any constraint.

Realistically, there may be changes in the phenology-environment coupling (Φ').

$$Y_{act} = \Phi'\left(\boldsymbol{X}_{new}\right) = \Phi(\boldsymbol{X}) + \left[\Phi'\left(\boldsymbol{X}_{new}\right) - \Phi(\boldsymbol{X})\right] = Y + \Delta Y_{act} \tag{4}$$

Here we refer to the observed phenology given $\boldsymbol{X}_{new}$ as the actual phenology (Y_{act}), and its difference from P as the actual phenological change (ΔY_{act}). The phenological mismatch (Y_{mis}) is then defined as the difference between Y_{act} and Y_{pot}. Its magnitude is related to the loss of synchronization, i.e., the extent to which Φ' deviates from Φ.

$$Y_{mis} = Y_{act} - Y_{pot} = \Delta Y_{act} - \Delta Y_{pot} \tag{5}$$

Estimating phenological mismatch on large spatial scales with empirical data

Data

Herbarium and climate data

In order to examine possible mismatch between plant phenology and climate change, we used a published crowdsourced dataset of plant reproductive phenology

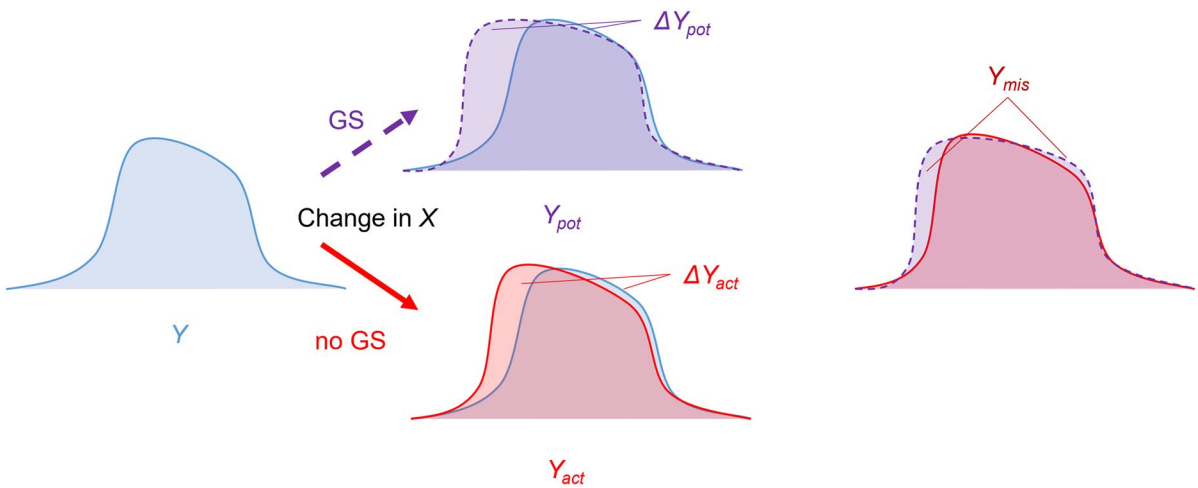

Fig. 3 With the change in the environmental factors ($\boldsymbol{X}$), the baseline phenology (Y) is expected to change to potential phenology (Y_{pot}) under generalized synchronization (GS) in the ideal case; in reality, however, it is observed to change to actual phenology (Y_{act}). The deviations from Y are referred to as potential and actual phenological change (ΔY_{act} and ΔY_{pot}), respectively. The difference between potential and actual phenology is defined as phenological mismatch (Y_{mis})

from herbarium specimens across the eastern continental United States spanning from 1895 to 2015 (Park et al. 2018) (Fig. 4a). Park et al. (2018) crowdsourced phenological data online from over 7,000 herbarium specimens representing 30 flowering plant species. Crowdsourcers classified the specimens into flowering and fruiting and each was given a reliability score. For specimens without accurate coordinates, they used county of specimen collection for locality information. Park et al. (2018) also retrieved auxiliary climatic data (monthly temperature and precipitation) from the PRISM dataset at 4 km resolution (PRISM Climate Group 2019). In this case study, we focused on the match between the flowering time (FT) (day of year) and spring mean temperature (SMT) (°C) defined as the mean of March, April, and May temperatures. We filtered out crowdsourcing records that were unreliable (reliability score = 0) and only kept one record for each specimen. We split the dataset into an early (prior to 1950) and a late (on or after 1950) period, and selected for species with no fewer than 30 records in both periods, leaving 19 species in our analysis.

Bird nestling ringing and climate data

To examine possible mismatch between bird breeding phenology and climate change, we used a published spatiotemporal dataset of over 820,000 nestling ringing records of 73 boreal bird species in Finland spanning from 1975 to 2017 (Hällfors et al. 2020) (Fig. 5a). As nestlings can only be ringed at a certain size, ringing dates are highly correlated with egg-laying dates, providing a high-quality indicator for the nestling ringing time (NRT) (day of year). The locations of nests were recorded at 10 × 10 km resolution. For each species, we aggregated nest-level NRT to the regional level by taking the median in 100 km diameter hexagons (Fig. 5a) to reduce the noise in data (Freeman et al. 2021). For each nest location, we retrieved auxiliary climatic data, mean annual temperature (MAT) (°C) from the TerraClimate dataset at ~ 4 km (1/24th degree) resolution (Abatzoglou et al. 2018). Similarly, we aggregated MAT by taking the median at all possible nest locations for a species and year in each hexagon. We removed hexagons with fewer than 50 nests with NRT data, leaving 28,017 records (hexagon × year). We split the dataset into an early (prior to 1995) and a late (on or after 1995) period, and selected for species with no fewer than 100 records in both periods, leaving 36 species in our analysis.

Methods

We preliminarily visualized the relationships between climatic and phenological data in the early and late period (Figs. 4b, 5b) to inspect the consistency in the climate-phenology functional relationship. We then systematically applied our prediction-based approach for each study system. We fitted a linear regression model between climatic and phenological variables (Eq. 6) to data in the early period only. In order to account for spatial autocorrelation among data points, we modeled spatial random effects with an exponential correlation function. We adopted a hierarchical Bayesian approach to build and fit the model, using the *spBayes* package in *R* (Finley et al. 2013).

$$
\begin{aligned}
&Y(s) = \beta_0 + \beta_1 X(s) + w(s) + \varepsilon \\
&w(s) \sim N(0, K) K_{ij} = \sigma^2 \exp(-\varphi \parallel s_i + s_j \parallel) \\
&\varepsilon \sim N(0, \tau^2) \\
&\begin{pmatrix} \beta_0 \\ \beta_1 \end{pmatrix} \sim MVN[\begin{pmatrix} 0 \\ 0 \end{pmatrix}, \begin{pmatrix} 100 & 0 \\ 0 & 100 \end{pmatrix}] \\
&\sigma^2 \sim lG(2, 2) \\
&\varphi \sim U(-\frac{\log(0.05)}{100d}, -\frac{\log(0.05)}{0.01d}) \\
&\tau^2 \sim IG(2, 0.1)
\end{aligned}
\tag{6}
$$

where the response variable Y is the phenological variable (FS in the plant case study and BS in the bird case study) and the covariates X is the climatic variable (SMT in the plant case study and MAT in the bird case study). β_0 and β_1 are the coefficients for intercepts and covariates; s is the location of observation (in longitude and latitude for the plant case study and easting and northing in EPSG:3067 projection for the bird case study); ε is the random error. The spatial random effect, w, is determined by the spatial variance parameter σ^2, the residual error variance τ^2, the spatial decay parameter φ, and the Euclidean distance between locations i and j. We empirically estimated d, the effective range of spatial dependence (Finley et al. 2015), by fitting an exponential function to the semivariograms of the residuals of the corresponding nonspatial linear regression models. We used common choices of diffuse multivariate normal (MVN) priors on β, a diffuse inverse gamma (IG) prios on σ^2 , a tight IG prior on τ^2, and a diffuse uniform (U) priors on φ (Finley et al. 2013). We ran the Markov chain Monte Carlo (MCMC) sampler (10,000 samples for the flowering case study and 1000 samples for the bird breeding

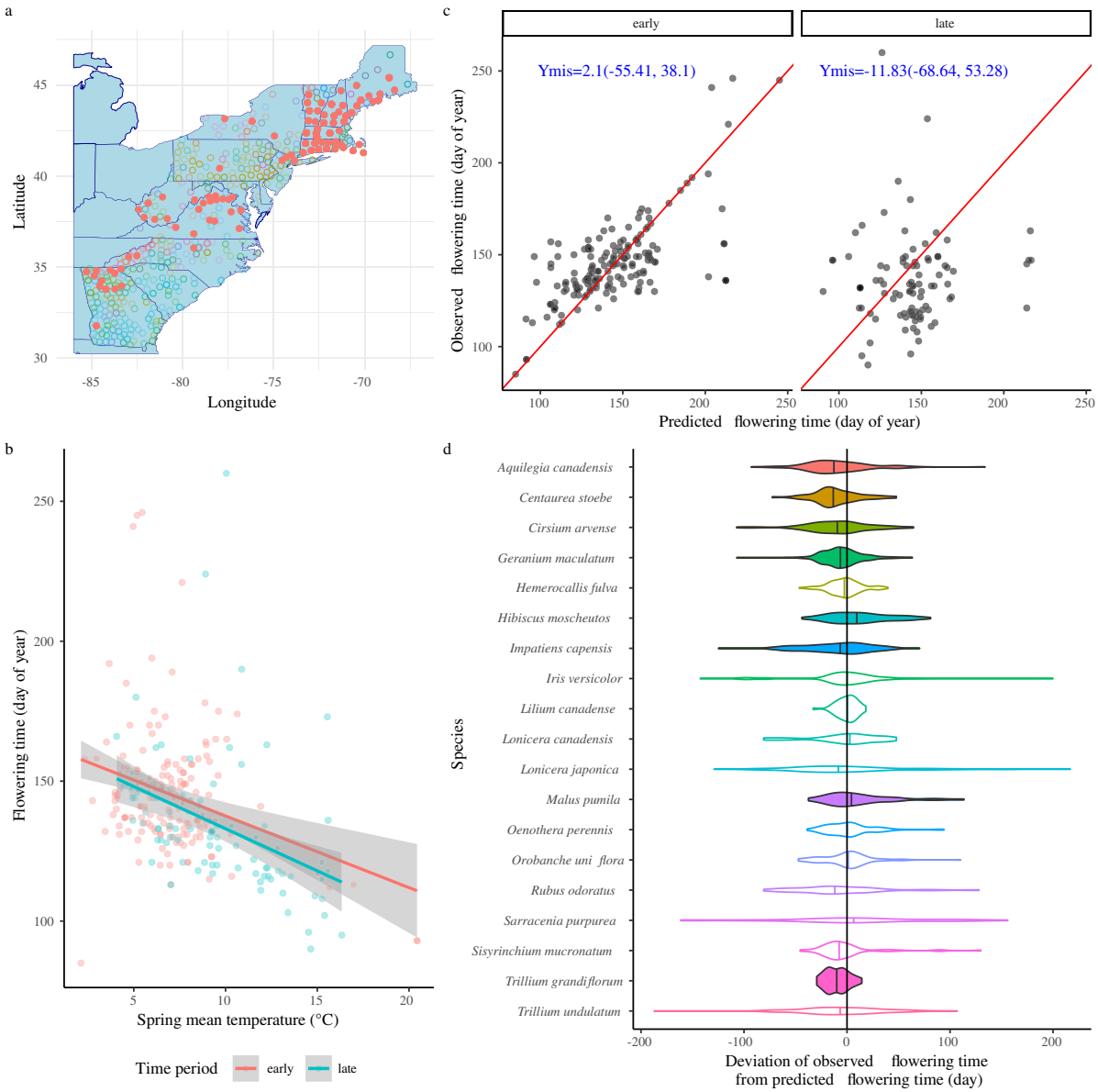

Fig. 4 **a** Geographical distribution of herbarium specimens from 19 plant species in the eastern United States. Data were originally published in Park et al. (2018). An example species, *Aquilegia canadensis*, is highlighted in solid dots. **b** Relationship between the flowering time (FT) and spring mean temperature (SMT) of *Aquilegia canadensis* in the early (before 1950) and late (on or after 1950) periods, respectively. Fitted lines and 95% standard errors are shown for each period. **c** Comparison between observed and predicted FT of *Aquilegia canadensis* in the early and late periods, respectively. 1:1 lines are shown in red. **d** Distribution of deviation of observed FT from predicted FT for each species. Species with deviations significantly different from zero are highlighted in solid

case study) (Finley et al. 2013), discarding the first half of the samples as burn-in.

We used the fitted model informed by data in the early period (X and Y) to predict phenological data in the early and late periods, respectively (Figs. 4c, 5c). Predictions were compared to observations in the early period to evaluate the model fit using the coefficient of determination (R^2) and root mean square error (RMSE). We similarly compared the predictions in the late period (Y_{pot}) with observations in the late period (Y_{act}) to estimate

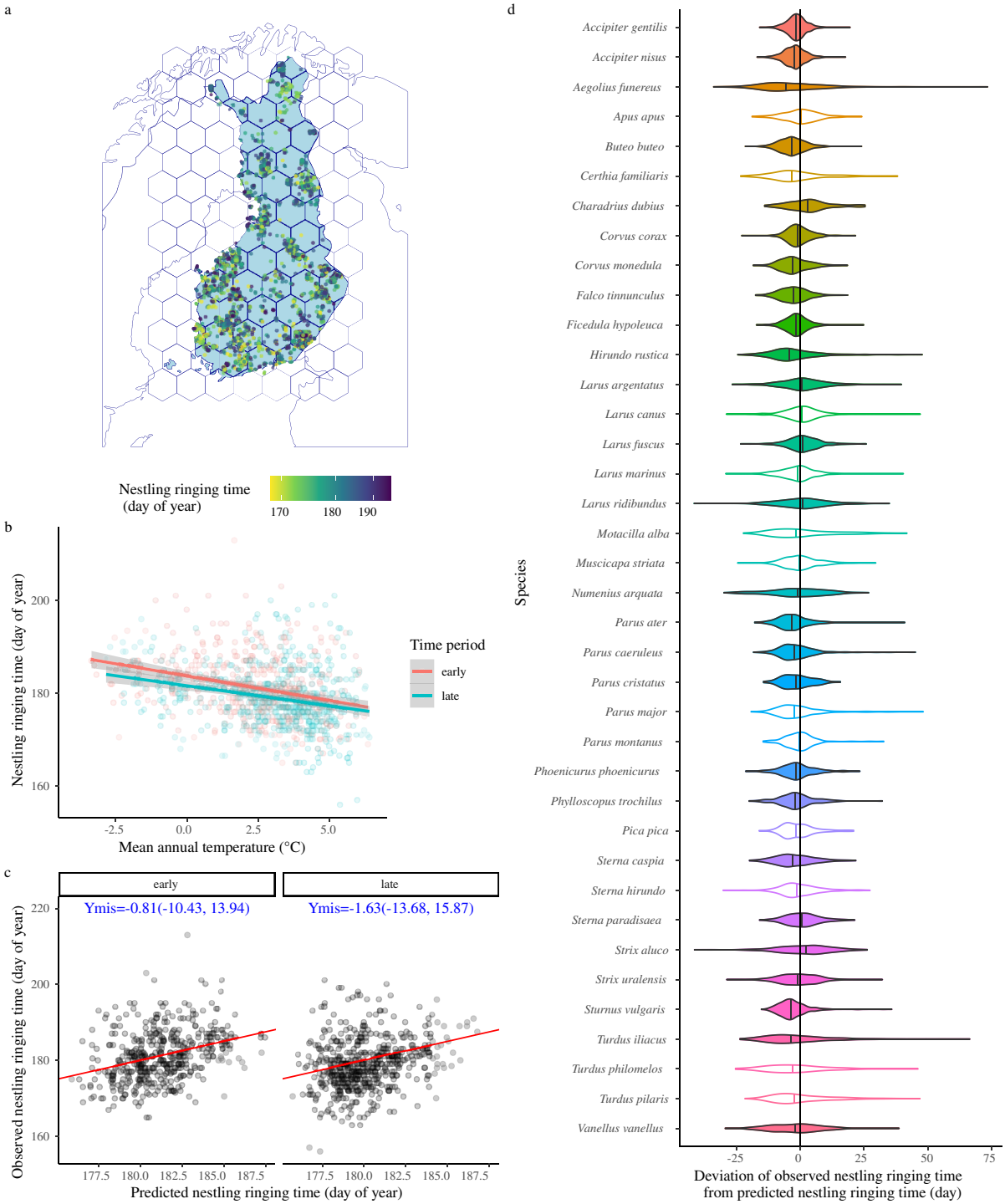
a
Nestling ringing time
(day of year)
170
180
190
b
Nestling ringing time (day of year)
200
180
160
-2.5
0.0
2.5
5.0
Mean annual temperature (°C)
Time period
early
late
c
early
late
Ymis=-0.81(-10.43, 13.94)
Ymis=-1.63(-13.68, 15.87)
Observed nestling ringing time (day of year)
220
200
180
160
177.5
180.0
182.5
185.0
187.5
Predicted nestling ringing time (day of year)
d
Species
Accipiter gentilis
Accipiter nisus
Aegolius funereus
Apus apus
Buteo buteo
Certhia familiaris
Charadrius dubius
Corvus corax
Corvus monedula
Falco tinnunculus
Ficedula hypoleuca
Hirundo rustica
Larus argentatus
Larus canus
Larus fuscus
Larus marinus
Larus ridibundus
Motacilla alba
Muscicapa striata
Numenius arquata
Parus ater
Parus caeruleus
Parus cristatus
Parus major
Parus montanus
Phoenicurus phoenicurus
Phylloscopus trochilus
Pica pica
Sterna caspia
Sterna hirundo
Sterna paradisaea
Strix aluco
Strix uralensis
Sturnus vulgaris
Turdus iliacus
Turdus philomelos
Turdus pilaris
Vanellus vanellus
-25
0
25
50
75
Deviation of observed nestling ringing time
from predicted nestling ringing time (day)

◂**Fig. 5** **a** Geographical distribution of bird nestling ringing events for an example species, *Phoenicurus phoenicurus*, out of 38 boreal bird species in Finland in this study. Data were originally published in Hällfors et al. (2020). Color of dots show the nestling ringing time (NRT) on the nest level. Data were aggregated to 100 km diameter hexagons for further analysis. **b** Relationship between NRT of *Phoenicurus phoenicurus* and mean annual temperature (MAT) in the early (before 1995) and late (on or after 1995) periods, respectively. Fitted lines and 95% standard errors are shown for each period. **c** Comparison between observed and predicted NRT of *Phoenicurus phoenicurus* in the early and late periods, respectively. 1:1 lines are shown in red. **d** Distribution of deviation of observed NRT from predicted NRT for each species. Species with deviations significantly different from zero are highlighted in solid

possible phenological mismatch. Specifically, we calculated and summarised the deviation between observations from predictions (Y_{mis}). We performed one-sample *t*-tests for each individual species to determine if the calculated mismatch was significantly different from zero. All calculations and statistical analyses were conducted in *R* v. 4.2.0 (R Core Team 2021).

Results

Advancement in flowering matches or outpaces spring warming in eastern US

Temperature niche (median SMT of all specimens) of all 19 species ranged from 6.06 to 16.0 °C. Phenological niche (median FT of all specimens) ranged from 129 to 228 day of year. There were significant correlations between FT and SMT in 17 out of 19 species, with FT being 2–5 days earlier with every 1 °C increase in temperature in these 17 species. When fitting linear models between FT and SMT in the early and late periods, respectively, the intercept changed slightly by − 0.815 (95% interval: − 36.5, 33.9) days and the slope changed slightly by 0.0684 (−3.39, 5.55) days/°C. Due to spatial bias in sampling and the difficulty of interpreting these parameter changes in linear models, we fitted spatial regression models to each species using data in the early period. For the early period, the fitted data had an R^2 of 0.465 (0.272, 0.819) and an RMSE of 21.0 (6.55, 49.2) days. For the late period, the predicted data had an R^2 of 0.0791 (0.00407, 0.507) and an RMSE of 32.6 (12.0, 65.8) days. The considerable reduction in model fit and increase in error for the late period suggest the loss of predictive skills in the climate-phenology model. The predicted FT in the later period deviated from the observed FT significantly in eight out of 19 species (Fig. 4d), with six species having observed FT significantly earlier ($p < 0.05$) than predictions by 5.00 to 14.4 days and two species significantly later by 1.84 to 10.9 days. The observations did not significantly differ from our predictions for most species (11 out of 19). The median of the residuals of all species was significantly lower than zero ($p < 0.05$), suggesting that this loss of predictive skills was not only from the process of extrapolation but also a possible change in the climate-phenology coupling over time.

Advancement in bird breeding slightly outpaces warming trends in most species in Finland

On the regional level (after aggregated to 100 km diameter hexagons), temperature niche (median MAT of all nests) of all 36 species ranged from 2.65 to 5.71 °C. Phenological niche (median NRT from all nests) ranged from 128 to 208 day of year. All 38 species experienced significant warming in their habitats from 1975 to 2017, with an increase in MAT ranging from 0.0461 to 0.0496 °C/year. In response to warming, 34 out of 38 species significantly advanced their NRT at a rate of

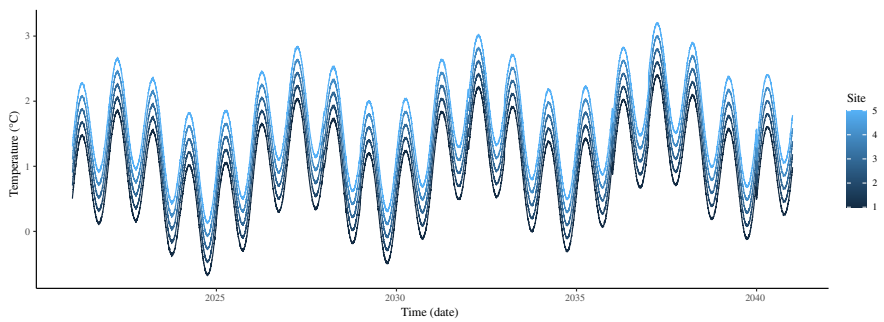

Fig. 6 Simulated temperature at five sites in a 20-year time period

0.045–0.258 days/year. There were significant correlations between NRT and MAT in all 38 species, with NRT being 0.78 to 4.17 days earlier with every 1 °C increase in temperature. When fitting linear models between NRT and MAT in the early and late periods, respectively, the intercept changed very slightly by 0.164 (-8.80, 8.44) days and the slope too by −0.221 (−1.47, 1.69) days/°C. We fitted spatial regression models to each species using data in the early period. For the early period, the fitted data had an R^2 of 0.188 (0.0601, 0.345) and an RMSE of 7.52 (4.89, 11.4) days. For the late period, the predicted data had an R^2 of 0.100 (0.00375, 0.355) and an RMSE of 7.55 (4.61, 12.9) days. The slight reduction in model fit and increase in error for the late period suggest loss in predictive skills similar to the previous case study, although to a smaller extent. The predicted NRT in the later period deviated from the observed NRT significantly in 26 out of 38 species (Fig. 4d), with 20 species having observed NRT significantly earlier than predictions by 0.964–5.80 days and four species significantly later by 0.665–3.20 days. For the remaining 12 species, the observations did not significantly differ from the predictions. The overall significant negative residual among all species ($p<0.05$) strongly suggests a change in the climate-phenology coupling over time.

Recovering phenological mismatch with simulated continuous phenology data

Methods

Simulate phenology during climate change

The two empirical case studies use empirical data on the annual temporal scale, such as the timing of flowering or hatching. Nevertheless, more characteristics in phenology curves, such as the starting time, peaking time, rate of change, and number of life cycles and their possible mismatch, can be examined using continuous data on finer temporal scales. Due to the difficulty to retrieve long-term continuous phenology data, we conducted four sets of simulation experiments to test the power of the proposed theoretical framework and methods in quantifying more nuanced phenological mismatch.

We first simulated hypothetical daily temperature curves at five sites in 20 years (January 1, 2021 to December 31, 2040) with an overall increasing linear trend, seasonal cycles, interannual fluctuations (Remsberg and Deaver 2005), and random noise (Eq. 7) (Fig. 6).

$$\begin{aligned} &X_s = \beta_{0,s} + \beta_{1,t} + A_1 \sin\left(\tfrac{2\pi}{\lambda_1}(t+\phi_1)\right) \\ &+A_2 \sin\left(\tfrac{2\pi}{\lambda_2}(t+\phi_2)\right) + \varepsilon_X \varepsilon_X \sim N(0,\sigma_X^2) \\ &\beta_{0,s} = 0.3 + 0.2s, \beta_1 = 0.0001 \\ &A_1 = 20, \lambda_1 = 365 \text{or} 366, \phi_1 = -\tfrac{1}{6} \\ &A_2 = 12, \lambda_1 = 5 \times (365 \text{or} 366), \phi_2 = 0 \end{aligned} \tag{7}$$

Here X_s stands for daily temperature, but it can be generalized to represent other environmental variables, t is time (day) since the start of the time period. The five sites are indexed with $s=1, \ldots, 5$, with increasing temperature from site 1 to 5. β_1 gives an overall increasing trend of 0.0001 °C/day, which is much faster than the recent observed warming of 0.08 °C/decade (Huang et al. 2017) in order to demonstrate our approach within a short time period.

We simulated hypothetical daily phenology each year as a double logistic curve, using a parameterization adapted from Elmore et al. (2012) (Eq. 8). This curve is commonly used to model ground-based and remotely-sensed leafing phenology (Zhang et al. 2006). A change was made to the original parameterization for this study in order to allow multiple growing seasons in a year (additional parameter m_8 for rescaling time depending on the number of life cycles per year).

$$\begin{aligned} &y = m_1 + (m_2 - m_7 d')\left(\frac{1}{1+\exp\left(\frac{m_3-d'}{m_4}\right)} - \frac{1}{1+\exp\left(\frac{m_5-d'}{m_6}\right)}\right) + \varepsilon_y \\ &d' = \left(d \bmod \tfrac{365}{m_8}\right) m_8 \\ &\varepsilon_y \sim N\left(0, \sigma_y^2\right) \end{aligned} \tag{8}$$

Here y is a variable that quantifies daily phenology (e.g., vegetation greenness, plankton abundance), d is time in Julian days, and m_1 to m_8 are parameters that determine the shape of the annual development curve (Table 1).

We extended Eq. 7 with hypothetical logistic relationships between the model parameters of year i (m_i) and a certain yearly summary ($X_{summ,i}$) of the environmental variable X (e.g., mean temperature in the first 90 days of a year) (Eq. 9).

$$m_i = \frac{L_{upper} - L_{lower}}{1 + \exp(-k(X_{summ,i} - X_0))} + L_{lower} \tag{9}$$

With Eqns. 7–9, we simulated phenology in 20 years under climate change assuming the same climate-phenology relationship. In order to simulate phenological

Table 1 Meanings of parameters in our adapted double logistic phenology model

Parameter	Meaning
m_1	Average value in winter
m_2	Difference between summer and winter
m_3	Timing of spring onset
m_4	Slope of curve in spring
m_5	Timing of fall offset
m_6	Slope of curve in fall
m_7	Slope of curve in summer
m_8	Number of life cycles (without rounding)

mismatch, we manually changed the values of m to be different from those generated by Eq. 9 in the second half of the time period, representing a change in the climate-phenology relationship. We generated phenology curves using both the unmodified and modified m, representing potential phenology (y_{pot}) and actual phenology (y_{act}), respectively.

To test the power of our approach in detecting multiple types of phenological mismatch, we manipulated four phenology model parameters: m_3 for mismatch in the timing of events (Fig. 7a), m_4 for mismatch in the pace of development (Fig. 7b), m_2 for mismatch in the intensity of activities (Fig. 7c), and m_8 for mismatch in the number of the life cycle (Fig. 7d).

Measure phenological mismatch

We first attempted to model the climate-phenology relationship using data from the first half of the time period. In practice, we do not know the critical environmental cues, the functional relationship between environmental cues and phenology model parameters, and even the correct structure of the phenology model. Commonly used phenology models often assume linear relationships between the timing of events and "critical environmental cues," such as growing degree-days and chilling units (Yun et al. 2017; Hufkens et al. 2018). However, in order to model continuous phenology data and detect mismatch in all parts of the life cycle, a more flexible model is needed.

Therefore, we used a state-of-the-art data-driven approach, empirical dynamic modeling (EDM), to model the nonlinear climate-phenology relationship (Sugihara and May 1990; Sugihara et al. 1994; Munch et al. 2017). According to Takens' theorem (Takens 1981), the time series of each variable contains information about all other variables in the same system. This theorem allows us to reconstruct the behavior of dynamical systems by taking the time-lag coordinates of the single variable as proxies for the other variables. In this study, we build on the Gaussian Process EDM (GP-EDM) algorithm initially applied to forecasting fish population dynamics (Munch et al. 2017). Operating with minimal assumptions, this approach holds the promise of revealing complex causal relationships from time series and outperforms parametric alternatives in prediction.

The model was set up as follows.

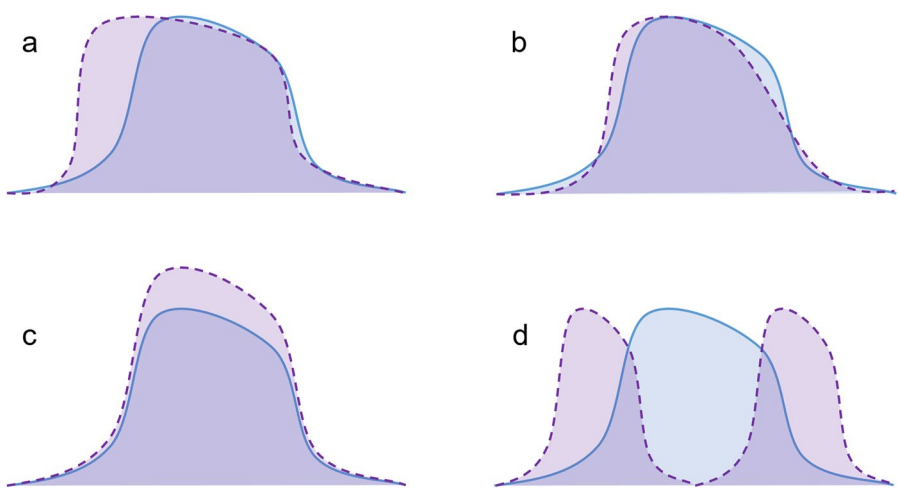

Fig. 7 Four types of phenological mismatch: **a** timing of events, **b** pace of development, **c** intensity of activities, and **d** number of life cycle

$$
\begin{aligned}
&p(y|g, \boldsymbol{X}, \varepsilon) \sim N\left(g\left(\boldsymbol{X'}\right), \varepsilon\right)\\
&p(g|\gamma) \sim GP\left(f, \sum_s\right)\\
&p(f|\omega) \sim GP\left(h, \sum_d\right)\\
&p\left(h|\phi, \tau^2\right) \sim GP\left(0, \sum_X\right)\\
&\sum_{s,ij} = \exp\left(-\frac{\gamma}{2}\left\|s_i - s_j\right\|^2\right)\sum_d\\
&\sum_{d,ij} = \exp\left(-\frac{\omega}{2}\left\|d_i - d_j\right\|^2\right)\sum_X\\
&\sum_{X,ij} = \tau^2\exp\left(-\frac{\phi}{2}\left|\boldsymbol{X'}_i - \boldsymbol{X'}_j\right|^2\right)\\
&\boldsymbol{X'} = \left(\overline{\boldsymbol{X}_{i,-1:14}}, \overline{\boldsymbol{X}_{i,-15:28}}, \ldots \overline{\boldsymbol{X}_{i,-337:364}}\right)
\end{aligned}
$$

$$
\begin{aligned}
&\mathrm{logit}\left(\frac{\phi_k - 1e^{-50}}{2\pi^2 - 1e^{-50}}\right) \sim N\left(0, 0.1\exp\left(-\frac{(\delta_k/365)^2}{5}\right)\right)\\
&\mathrm{logit}\left(\frac{\varepsilon - 0.001}{0.0615 - 0.001}\right) \sim N(0, 0.5)\\
&\mathrm{logit}\left(\frac{\tau^2 - 0.001}{0.0615 - 0.001}\right) \sim N(0.0625, 50)\\
&\mathrm{logit}\left(\frac{\omega - (1/30)^2}{1 - (1/30)^2}\right) \sim N(0, 0.5)\\
&\mathrm{logit}\left(\frac{\gamma - (1/100)^2}{(1/0.01)^2 - (1/100)^2}\right) \sim N(0, 0.5)
\end{aligned}
\tag{10}
$$

For each GP distribution, we assume that the predicted function values and observed data points (also called basis) have a jointly multivariate normal distribution with a covariance matrix determined by the similarity in predictors. The environmental predictor $\boldsymbol{X}$' for a specific site and time is a vector of time-lagged $\boldsymbol{X}$, consisting of 26 of 14-day averages in the past 364 days. A baseline functional relationship h between y and $\boldsymbol{X}$' is a GP parameterized by point-wise-prior variance in the function τ^2 and lag-specific length-scale parameters $\phi_{1:26}$. The functional relationship is more similar at closer day of year (the degree of similarity controlled by ω) and at closer sites (the degree of similarity controlled by γ). The process variance is ε. Informed priors were imposed on transformed parameters, with δ_k indicating the temporal distance of the k-th predictor to the data point.

We initialized five sets of random EDM parameters with the prior distribution. With training data in the first ten years, we optimized these five sets of EDM parameters with stochastic backpropagation (Riedmiller and Braun 1993), giving rise to a model ensemble with five members. Using this model ensemble, we predict the phenology in the whole time period, including the potential phenology under climate change in the late period (y_{pot}'). The estimated phenological mismatch (y_{mis}') was calculated as the difference between observed mismatched phenology and predicted potential phenology in the late period.

$$
y'_{mis} = y_{act} - y'_{pot} \tag{11}
$$

This estimate was compared to the simulated phenological mismatch (y_{mis}), which was the difference between observed mismatched phenology and simulated potential phenology.

$$
y_{mis} = y_{act} - y_{pot} \tag{12}
$$

We used normalized RMSE to summarize the overall phenological mismatch. Here we normalized the RMSE to a percentage of the range of training phenology data (i.e., y in the first 10 years). This metric describes how much the observed mismatched phenology deviates from the potential phenology expected with the same climate-phenology relationship.

$$
\begin{aligned}
\Delta'_{\mathrm{mis}} &= \frac{\sqrt{\frac{1}{N}\sum_{i=1}^{n}\left(y_{act} - y'_{pot}\right)^2}}{max(y) - min(y)}\\
\Delta_{\mathrm{mis}} &= \frac{\sqrt{\frac{1}{N}\sum_{i=1}^{n}\left(y_{act} - y_{pot}\right)^2}}{max(y) - min(y)}
\end{aligned}
\tag{13}
$$

To evaluate the goodness-of-fit of our GP-EDM, we calculated the normalized RMSE between predicted phenology (y_{pot}') and simulated phenology (y_{pot}). This metric is also the difference between estimated and simulated phenological mismatch.

$$
\Delta_{\mathrm{error}} = \frac{\sqrt{\frac{1}{N}\sum_{i=1}^{n}\left(y - y'\right)^2}}{max(y) - min(y)} \tag{14}
$$

Results

Experiment 1: Timing of events

Shifts in the timing of spring phenological events, such as migration and breeding, are widespread in animals. A meta-analysis has shown an overall significant advancement by 2.88 days per decade in the timing of spring events since 1950 (Cohen et al. 2018), although delays have also been found in individual studies (Cohen et al. 2018). It has been a concern whether these phenological shifts in the timing

of events can cause phenological mismatches among interacting species and between the species and the environment (Cohen et al. 2018). In this experiment, we simulated breeding activities, with the timing of spring onset increasing with the mean daily temperature of the last 90 days in the previous year ($T_{\text{-90:-1}}$) (Fig. 8a). We further assumed that the mismatched phenology has later spring onset compared to the expected timing (Fig. 8b).

Our data-driven model accurately characterized how temperature cue controls the timing of spring onset of breeding activities (Fig. 8c, d). The estimated mismatch was close to the simulated mismatch and was larger in magnitude compared to the model predictive error (Fig. 8e). In the late period, the overall phenological mismatch was estimated to be $\Delta_{\text{mis}}' = 0.108$, comparable to the simulated value $\Delta_{\text{mis}} = 0.130$, and larger than the model predictive error $\Delta_{\text{error}} = 0.0500$.

Experiment 2: Pace of development

In plant phenology literature, there has been a trend to focus on not only discrete events but the continuous development, such as the speed of vegetation leaf development (Clark et al. 2011). Studies using remote

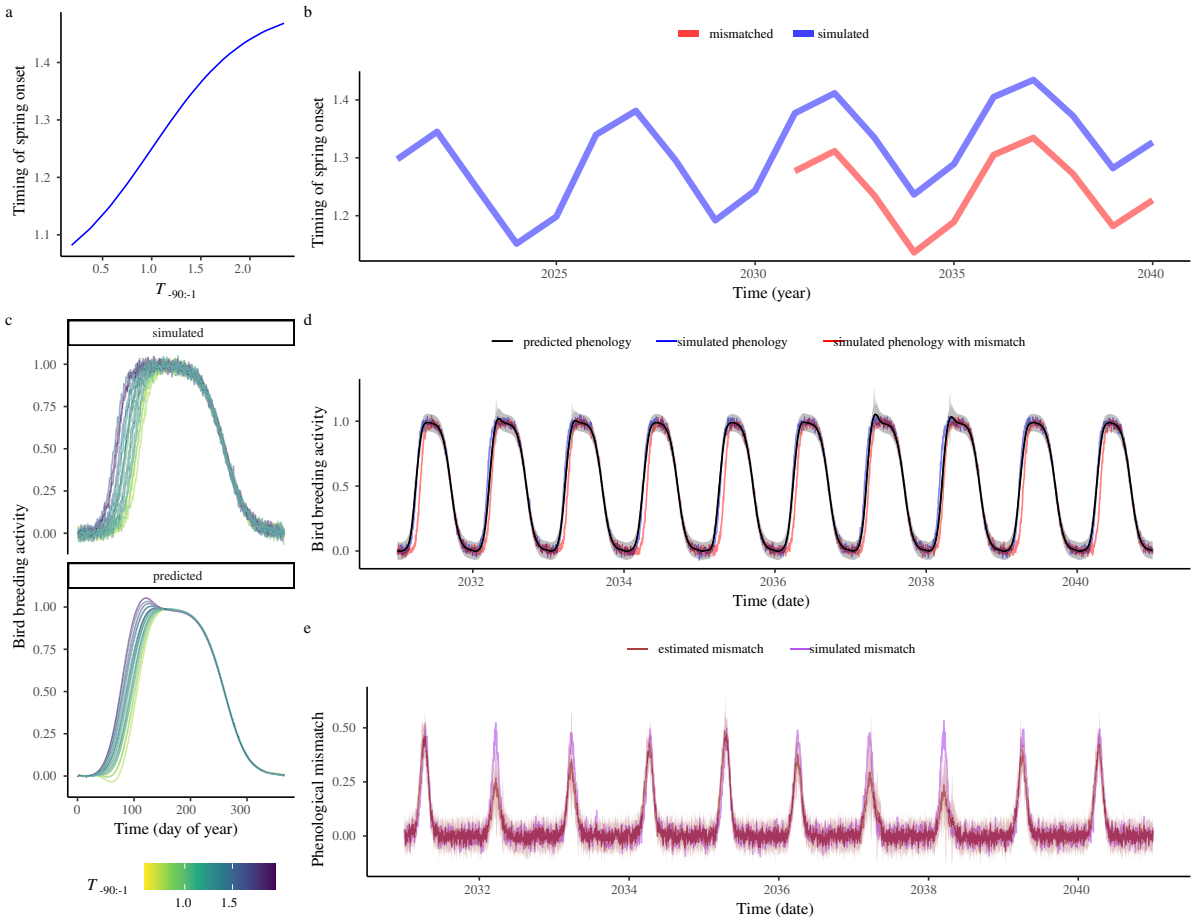

Fig. 8 Measuring phenological mismatch in the timing of events. **a** Functional relationship between the timing of spring onset (m_3) and the mean daily temperature of the last 90 days in the previous year ($T_{\text{-90:-1}}$). **b** Simulated and mismatched timing of spring onset (m_3). **c** The influence of mean daily temperature of the last 90 days in the previous year ($T_{\text{-90:-1}}$) on the simulated and model-predicted breeding activity in a year. **d** Time series of simulated breeding activity (blue), mismatched breeding activity (red), and predicted breeding activity (black). **e** Simulated phenological mismatch (purple) and estimated phenological mismatch (dark red). The ribbons around predicted phenology in **d** and estimated mismatch in **e** indicate estimated 95% confidence intervals

sensing have found that spring green-up is accelerated in years with higher temperature (Seyednasrollah et al. 2018) or with faster spring warming (Qiu et al. 2020). The sensitivity of the speed of spring green-up to temperature anomaly appeared to differ among cold, normal, and hot years (Seyednasrollah et al. 2018), but it has not been assessed whether there exists any phenological mismatch. In this experiment, we simulated leaf development characterized by enhanced vegetation index (EVI), with the speed of spring green-up increasing with the mean daily temperature of the first 14 days in the same year ($T_{1:14}$) (Fig. 9a). We further assumed that the mismatched phenology has slower spring green-up compared to the expected speed (Fig. 9b).

The model accurately characterized how temperature cue controls the pace of spring greenup (Fig. 9c, d). The estimated mismatch was close to the simulated mismatch and was larger in magnitude compared to the model predictive error (Fig. 9e). In the late period, the overall phenological mismatch was estimated to be $\Delta_{mis}' = 0.104$, comparable to the simulated value $\Delta_{mis} = 0.101$, and larger than the model predictive error $\Delta_{error} = 0.0370$.

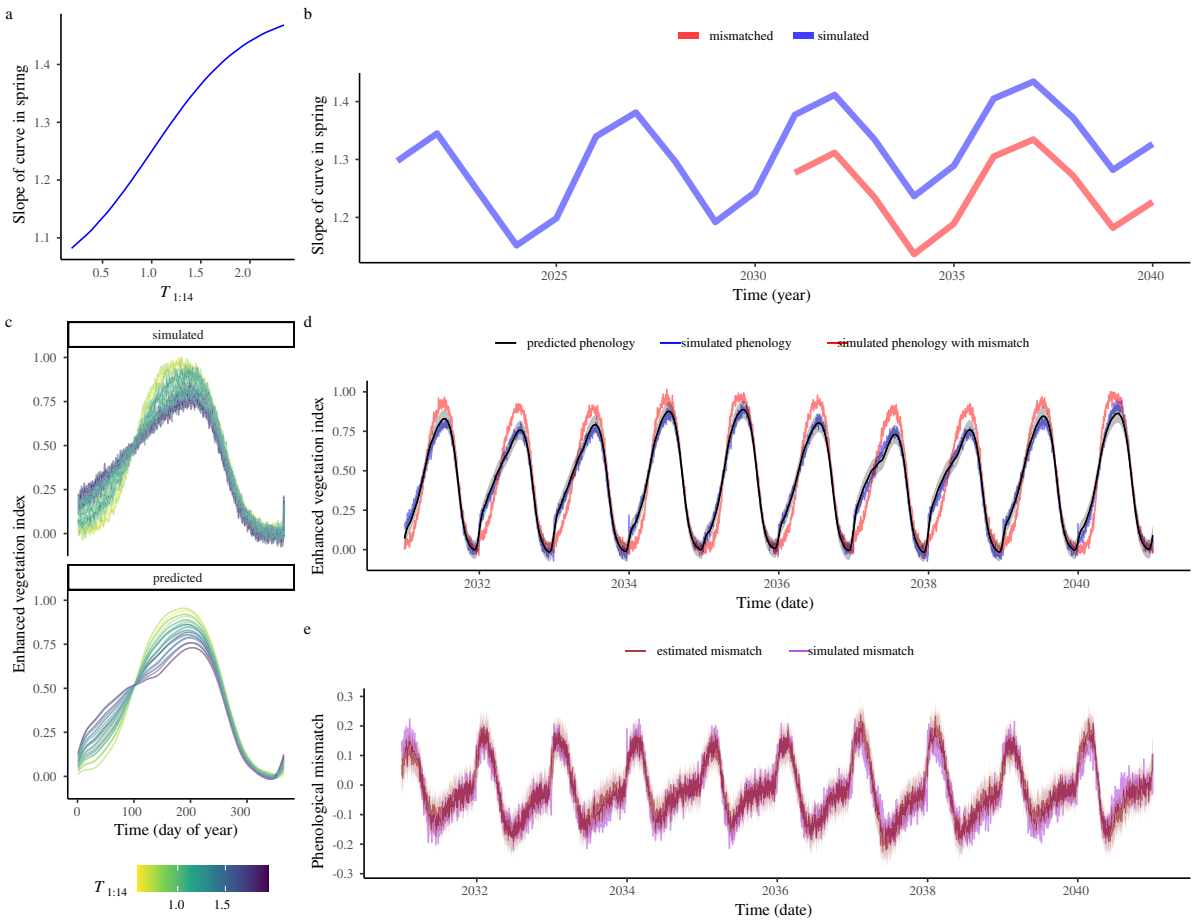

Fig. 9 Measuring phenological mismatch in the pace of development. **a** Functional relationship between the slope of curve in spring (m_4) and the mean daily temperature of the first 14 days in the same year ($T_{1:14}$). **b** Simulated and mismatched slope of curve in spring (m_4). **c** The influence of mean daily temperature of the first 14 days in the same year ($T_{1:14}$) on the simulated and model-predicted EVI in a year. **d** Time series of simulated EVI (blue), mismatched EVI (red), and predicted EVI (black). **e** Simulated phenological mismatch (purple) and estimated phenological mismatch (dark red). The ribbons around predicted phenology in **d** and estimated mismatch in **e** indicate estimated 95% confidence intervals

Experiment 3: Intensity of activities

On the ecosystem level, it has been shown that there is a trade-off between length of the growing season and peak net primary productivity (NPP) (Duveneck and Thompson 2017). In warmer years, there are often longer growing seasons but lower summer NPP. This trade-off has been well documented but only described with simple statistical models. It is, therefore, hard to determine if changes in productivity track climate change. Using our approach, we consider the continuous change of NPP as phenology on the ecosystem level and quantify the mismatch with temperature. In this experiment, we simulated NPP, with the peak NPP increasing with the mean daily temperature of the first 90 days in the same year ($T_{1:90}$) (Fig. 10a). We further assumed that the mismatched phenology has a lower peak NPP compared to the expected intensity (Fig. 10b).

The model accurately characterized how temperature cue controls the peak NPP (Fig. 10c and d). The estimated mismatch was close to the simulated mismatch and was larger in magnitude compared to the model predictive error (Fig. 10e). In the late period, the overall phenological mismatch was estimated to be $\Delta_{mis}' = 0.0857$, comparable to the simulated value

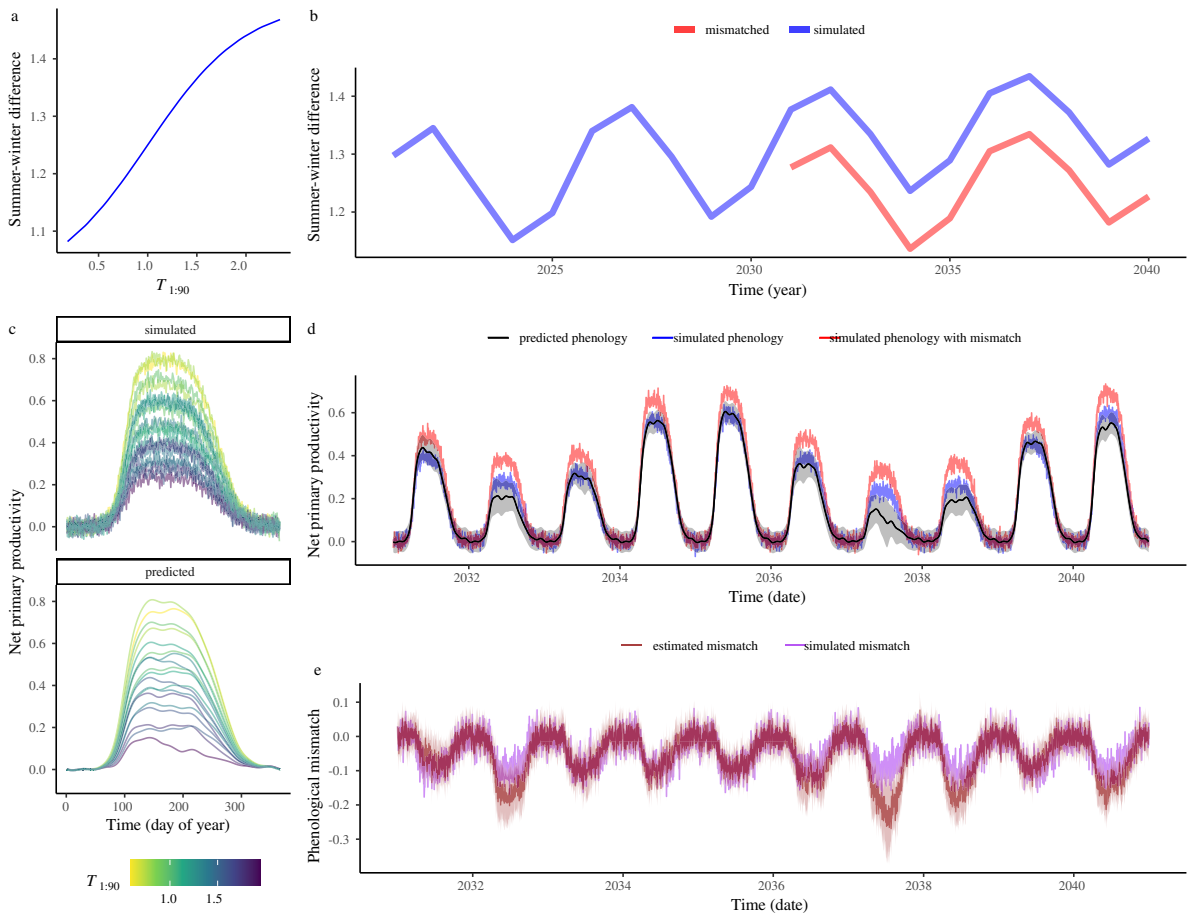

Fig. 10 Measuring phenological mismatch in the intensity of activities. **a** Functional relationship between the difference between summer and winter (m_2) and the mean daily temperature of the first 90 days in the same year ($T_{1:90}$). **b** Simulated and mismatched difference between summer and winter (m_2). **c** The influence of mean daily temperature of the first 90 days in the same year ($T_{1:90}$) on the simulated and model-predicted NPP in a year. **d** Time series of simulated NPP (blue), mismatched NPP (red), and predicted NPP (black). **e** Simulated phenological mismatch (purple) and estimated phenological mismatch (dark red). The ribbons around predicted phenology in **d** and estimated mismatch in **e** indicate estimated 95% confidence intervals

$\Delta_{mis} = 0.0740$, and larger than the model predictive error $\Delta_{error} = 0.0409$.

Experiment 4: Life history

Climate change can cause more complex changes in phenology, such as a change in life history. Several insect taxa, such as Lepidoptera species and bark beetles, have been found to complete more generations per year over time (from univoltine to bivoltine or multivoltine life cycles). These changes have been attributed to longer and warmer growing seasons (Forrest 2016). Many of these changes are economically important, especially when the insects are pests or parasites (Jönsson et al. 2009). Previous studies have taken a phenological perspective to study the synchrony between plants, pests, and parasites, leading to diverse findings on phenological mismatch (Senior et al. 2020). Nevertheless, it has rarely been assessed how changes in life history induce phenological mismatch. In this experiment, we simulated insect abundance, with the number of life cycles (without rounding) increasing with the mean daily temperature of all days in the same year ($T_{1:365}$) (Fig. 11a). We further assumed that the mismatched phenology has a

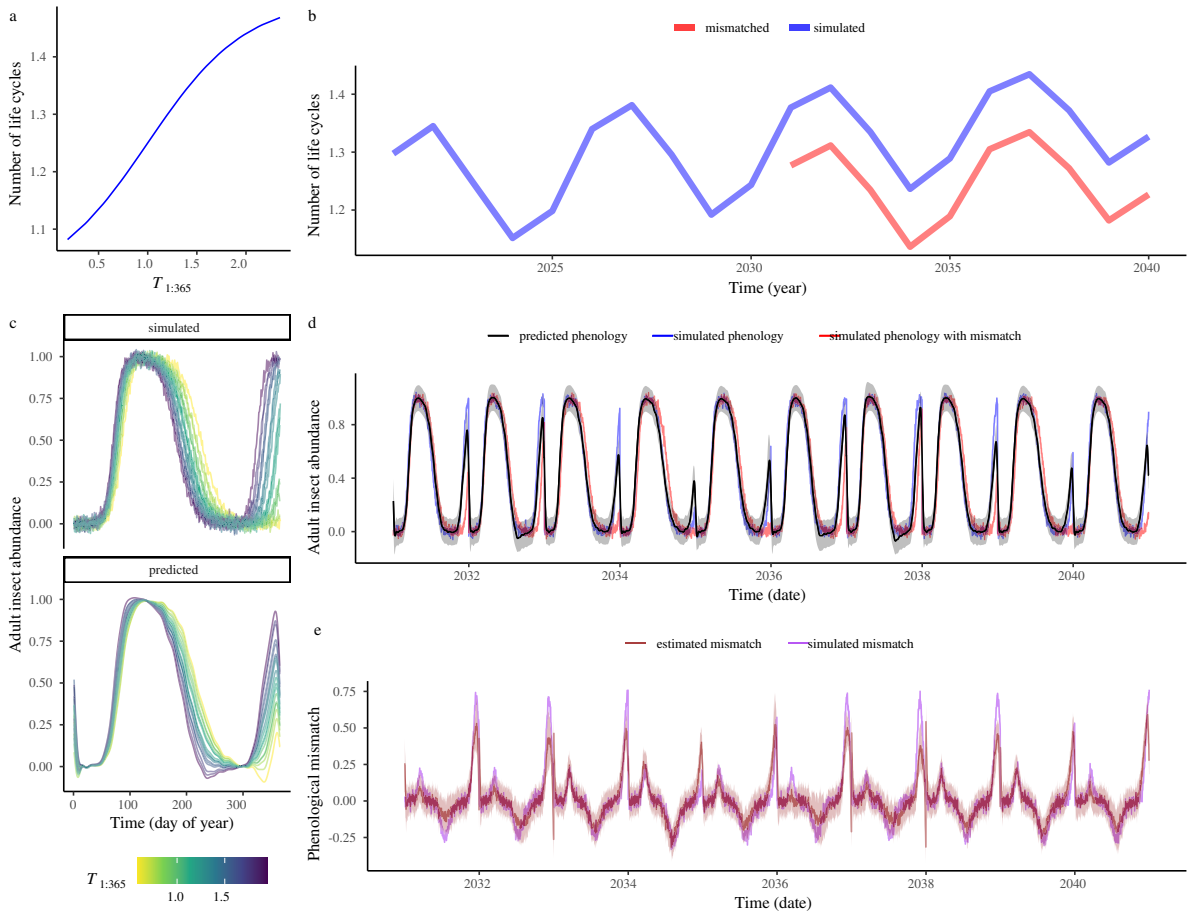

Fig. 11 Measuring phenological mismatch in life history. **a** Functional relationship between the number of life cycles (without rounding) (m_8) and the mean daily temperature of all days in the same year ($T_{1:365}$). **b** Simulated and mismatched number of life cycles (without rounding) (m_8). **c** The influence of mean daily temperature of all days in the same year ($T_{1:365}$) on the simulated and model-predicted insect abundance in a year. **d** Time series of simulated insect abundance (blue), mismatched insect abundance (red), and predicted insect abundance (black). **e** Simulated phenological mismatch (purple) and estimated phenological mismatch (dark red). The ribbons around predicted phenology in **d** and estimated mismatch in **e** indicate estimated 95% confidence intervals

lower number of life cycles compared to the expected intensity (Fig. 11b).

The data-driven nonlinear model relatively accurately characterized how increasing temperature accelerates the pace of development thus increasing the number of life cycles (Fig. 11c and d). The estimated mismatch was close to the simulated mismatch, and was larger in magnitude compared to the model predictive error (Fig. 11e). In the late period, the overall phenological mismatch was estimated to be $\Delta_{mis}' = 0.136$, comparable to the simulated value $\Delta_{mis} = 0.172$, and larger than the model predictive error $\Delta_{error} = 0.0831$.

Discussion

In this work, we sought to improve our understanding of phenological mismatch by (1) reviewing and classifying existing methods used to quantify phenological mismatch, (2) proposing a generalizable definition of synchrony and a predictive approach for quantification, and (3) quantifying phenological mismatch on large spatial scales under climate change using empirical and simulated data.

Despite the increasing research on phenological research on large scales, we have not yet seen a study that links phenological mismatch across multiple scales. This may be because the concept of phenological mismatch has been applied differently on different levels of the organization. For example, the population-level definition in the Cushing match-mismatch hypothesis, i.e., any change to the relative timing between the peak of the most energetically demanding period of the consumer and the peak of resource availability (Cushing 1969), can hardly be applied to another level of the organization. Our more general framework and approach may enable future studies that compare or even scale phenological mismatch across scales.

Compared to existing descriptive and model-comparison approaches, our predictive approach has the following advantages. First, we allow very flexible modeling of the baseline phenology-environment coupling, such as linear relationship in the empirical case studies and nonlinear relationship in the simulated case studies. Multivariate models can be used when phenology studied is controlled by complex mechanisms (e.g., grasslands) (Shen et al. 2011). In cases when asynchrony is a historical baseline prior to climate change (Singer and Parmesan 2010; Visser et al. 2012), models can be designed accordingly to represent increased synchrony as a type of phenological mismatch. Second, the resulting measure of phenological mismatch has the same unit as the phenological data, and can be normalized to a percentage, enabling easy interpretation and comparison across scales. The magnitude of phenological mismatch can therefore be quantitatively compared across scales. Third, we allow the analysis of continuous phenological curves without identifying critical features of phenological time series, making the approach generalizable to diverse study systems. This is particularly useful in systems with weak or cryptic seasonality (e.g., evergreen forests) (Wu et al. 2017; Abernethy et al. 2018), irregular periodicity (e.g., drought-controlled forests) (Killmann and Thong 1995; Borchert 1996), or more than one cycle per year (e.g. crops and insects) (Meza et al. 2008; Seifert and Lobell 2015; Forrest 2016).

Two empirical case studies showcased how the predictive approach can be applied to large spatiotemporal datasets to systematically quantify phenological mismatch. In the eastern US, we found plant flowering phenology to generally match or even outpace the increase in spring temperature from 1895 to 2015. This finding is consistent with a previous finding on the rapid advancement of plant spring phenology outpacing the shift in the spring timing, defined as the timing when temperature increases most rapidly in a year (Ovaskainen et al. 2013). In a continental-scale study using remote sensing data, land surface phenology also outpaced changes in mean annual temperature in natural landscapes in the eastern US (Song et al. 2021). These results suggest that plant flowering phenology in many species responds sensitively to warming and may even be mismatched in an unexpected direction. Advancing of spring phenology beyond the extent of warming might expose plants to extreme weather conditions such as frost (Richardson et al. 2018). There are several possible reasons for such outpacing phenological mismatch. First, the late period we defined in this case study (1950–2015) has much overlap with the "global warming hiatus" (Medhaug et al. 2017), such that the advancement in plant phenology may appear to be overcompensating. Second, although plant phenology responds to climate change through both phenotypic plasticity and

adaptive evolution, directional selection may be more dominant (Anderson et al. 2012), such that advanced phenology may not respond rapidly to the slowdown of warming. Third, although our case study spanned around 120 years, it is still a limitation that climate change has taken place during the early period that we defined (1895–2014) (Masson-Delmotte 2018). The baseline climate-phenology coupling we inferred from this period may still not represent a status without phenological mismatch. Last, phenology may be more strongly controlled by extreme weather conditions rather than mean temperatures (Crabbe et al. 2016). It is common that phenology shifts to match some climatic conditions but not the others. For example, tree swallows that advanced their egg laying in response to warming expose their offspring to more harsh weather events which reduced food availability (Shipley et al. 2020). Therefore, better mechanistic understanding is needed to identify the most ecologically relevant climate-phenology coupling for the quantification of phenological mismatch.

We focused on phenological mismatch on higher trophic levels in the bird breeding case study. We found a very similar pattern to the plant flowering case study in Finland, where the advancement of bird breeding season slightly but significantly outpaced warming. Although there have been many examples of bird reproductive phenology changing insufficiently in response to changes in climate or plant phenology (Visser et al. 1998; Both and Visser 2001; Gaston et al. 2009; Burger et al. 2012; Clausen and Clausen 2013; Mayor et al. 2017; Descamps et al. 2019; MacKenzie et al. 2019; Merkel et al. 2019), there are considerable variation among species (Dunn and Møller 2014) and study area. In this case study, it is not completely surprising that bird breeding phenology advanced more than expected given climate change, given that bird breeding phenology is often strongly coupled with spring vegetation greenness (La Sorte and Graham 2020), and that Finland land surface phenology seem to be outpacing warming in the last three decades (Song et al. 2021). This finding may be region-specific and therefore does not support the general opinion that lagging phenological mismatch is greater on higher trophic levels. A meta-analysis involving various terrestrial, freshwater, and marine taxa suggests differential phenological change among trophic levels, with secondary consumers having the slowest advancement in timing (Thackeray et al. 2010). The constraint of the phenological shift in higher-level consumers, and thus growing phenological mismatch with their resources, has also been suggested in terrestrial food webs (Both et al. 2009). More long-term datasets on the phenological relationship across trophic levels will help to examine these claims more systematically.

The accuracy of the proposed measure requires reasonable predictive power of the phenology model and is, therefore, sensitive to model structure. The better we can predict potential phenology during climate change, the better we can estimate phenological mismatch. Our experiments with simulated data demonstrated the accuracy of predicting phenological response under climate change and quantifying varying types of phenological mismatch. Nevertheless, the estimated phenological mismatch might be confounded by the loss of predictive skill that is expected during extrapolation, due to the variance in data and imperfect model fitting rather than a true phenological mismatch. Although phenological mismatch was shown to be a lot greater than model predictive error to estimated mismatch in the simulated studies, it is often not possible to assess the true predictive errors in the hypothetical scenario without phenological mismatch in empirical data. It is then helpful to conduct out-of-sample tests with a random subset of the data to understand model performance (see supplementary information). It is necessary to interpret the estimated phenological mismatch with care, considering the following caveats.

(1) When high-quality continuous phenology data are not available, there will not be sufficient information to determine the environment-phenology relationship, making it difficult to estimate phenological mismatch based on model predictions.
(2) Without a reasonable model structure for the environment-phenology relationship, the estimate of phenological mismatch can be incorrect and misleading. We here demonstrate that even using a nonlinear data-driven model, the performance when recovering highly complex climate-phenology coupling could still be limited, as shown in the simulation experiment 4 on life history. The GPEDM we used also suffers from limitations of modeling threshold effects or extrapolating to extreme conditions. Therefore, we suggest continuous searching and improvement of predictive

models, such as through integrating mechanistic knowledge into data-driven models (Read et al. 2019).

(3) If climate change has driven the environmental conditions out of the historical range, it is difficult to define what phenological response is tracking and what is mismatched with the environment. In our simulation experiments, we apply a space-for-time substitution, using data from sites with temperature differences to inform phenology in a wide range of environmental conditions in history. Alternatively, manipulative experiments might inform the expected behavior under unprecedented conditions.

(4) The estimated phenological mismatch is subjective to the choice of time periods compared. Although it would be ideal to set a baseline for climate-phenology coupling using data prior to anthropogenic climate change (Abram et al. 2016), such data are usually not available. Here we demonstrated our approach in the empirical studies by splitting a long-term dataset into an early and a late period. We need to interpret the estimated phenological mismatch relative to the time scale of the dataset, acknowledging that a comparison to the pre-industrial conditions may not be fully achieved.

(5) At the current stage, it has not been experimentally or empirically validated if our measure of phenological mismatch is linked to fitness or demographic consequences. Nevertheless, as it can detect several individual types of phenological mismatch that have verified consequences (e.g., in timing of events), we are optimistic that our proposed measure is ecologically meaningful.

Acknowledgements Y. Song was supported by the UCSC Hammett Fellowship and Microsoft Azure AI for Earth grant. K. Zhu was supported by the UCSC Committee on Research Faculty Research Grant and NSF Awards 1926438, 2306198 (CAREER).

Author contributions All authors contributed to the study conception and design. Data analyses were performed by YS. Methods of Gaussian Process empirical dynamic modeling was developed by SBM. The draft of the manuscript was written by YS and all authors commented and edited. All authors read and approved the final manuscript.

Funding Y. Song was supported by the UCSC Hammett Fellowship and Microsoft Azure AI for Earth grant. K. Zhu was supported by the UCSC Committee on Research Faculty Research Grant and NSF Awards 1926438, 2306198 (CAREER).

Data availability We used published and publicly available raw data in all case studies. Plant reproductive phenology data from herbarium specimens in the eastern continental United States (Park et al. 2018) are available from the Harvard Forest Data Archive (HF309): https://harvardforest1.fas.harvard.edu/exist/apps/datasets/showData.html?id=HF309. Bird nestling ringing data in Finland (Hällfors et al. 2020) are available from Dryad: https://doi.org/10.5061/dryad.wstqjq2ht. TerraClimate data (Abatzoglou et al. 2018) are available from the data catalog of the Climatology Lab: https://www.climatologylab.org/terraclimate.html. The fully reproducible workflow, including code and data, is available on Zenodo (https://doi.org/10.5281/zenodo.7553656).

Declarations

Competing interests The authors have no relevant financial or non-financial interests to disclose.

References

Abarbanel HDI, Rulkov NF, Sushchik MM (1996) Generalized synchronization of chaos: the auxiliary system approach. Phys Rev E 53(5):4528–4535

Abatzoglou JT, Dobrowski SZ, Parks SA, Hegewisch KC (2018) TerraClimate, a high-resolution global dataset of monthly climate and climatic water balance from 1958–2015. Sci Data. https://doi.org/10.1038/sdata.2017.191

Abernethy K, Bush ER, Forget P-M, Mendoza I, Morellato LPC (2018) Current issues in tropical phenology: a synthesis. Biotropica 50(3):477–482

Abram NJ, McGregor HV, Tierney JE, Evans MN, McKay NP, Kaufman DS (2016) Early onset of industrial-era warming across the oceans and continents. Nature 536(7617):411–418

Adrian R, Wilhelm S, Gerten D (2006) Life-history traits of lake plankton species may govern their phenological response to climate warming. Glob Change Biol 12(4):652–661

Aikens EO, Monteith KL, Merkle JA, Dwinnell SPH, Fralick GL, Kauffman MJ (2020) Drought reshuffles plant phenology and reduces the foraging benefit of green-wave surfing for a migratory ungulate. Glob Change Biol 26(8):4215–4225

Anderson JT, Inouye DW, McKinney AM, Colautti RI, Mitchell-Olds T (2012) Phenotypic plasticity and adaptive evolution contribute to advancing flowering phenology in response to climate change. Proc: Biol Sci 279(1743):3843–3852

Bartomeus I, Ascher JS, Wagner D, Danforth BN, Colla S, Kornbluth S, Winfree R (2011) Climate-associated

phenological advances in bee pollinators and bee-pollinated plants. Proc Natl Acad Sci 108(51):20645–20649
Beard KH, Kelsey KC, Leffler AJ, Welker JM (2019) The missing angle: ecosystem consequences of phenological Mismatch. Trends Ecol Evol. https://doi.org/10.1016/j.tree.2019.07.019
Blondel J, Maistre M, Perret P (1993) Habitat heterogeneity and life-history variation of Mediterranean blue tits (Parus caeruleus). Auk 110(3):511–520
Boccaletti S, Kurths J, Osipov G, Valladares DL, Zhou CS (2002) The synchronization of chaotic systems. Phys Rep 366(1–2):1–101
Borchert R (1996) Phenology and flowering periodicity of Neotropical dry forest species: evidence from herbarium collections. J Trop Ecol 12(1):65–80
Both C, Visser ME (2001) Adjustment to climate change is constrained by arrival date in a long-distance migrant bird. Nature 411(6835):296
Both C, Asch MV, Bijlsma RG, Burg ABVD, Visser ME (2009) Climate change and unequal phenological changes across four trophic levels: constraints or adaptations? J Anim Ecol 78(1):73–83
Brown R, Kocarev L (2000) A unifying definition of synchronization for dynamical systems. Chaos: an Interdisciplinary J Nonlinear Sci 10(2):344–349
Burger C, Belskii E, Eeva T, Laaksonen T, Mägi M, Mänd R, Qvarnström A, Slagsvold T, Veen T, Visser ME, Wiebe KL, Wiley C, Wright J, Both C (2012) Climate change, breeding date and nestling diet: How temperature differentially affects seasonal changes in pied flycatcher diet depending on habitat variation. J Anim Ecol 81(4):926–936
Burthe S, Daunt F, Butler A, Elston DA, Frederiksen M, Johns D, Newell M, Thackeray SJ, Wanless S (2012) Phenological trends and trophic mismatch across multiple levels of a North Sea pelagic food web. Mar Ecol Prog Ser 454:119–133
Clark JS, Agarwal P, Bell DM, Flikkema PG, Gelfand A, Nguyen X, Ward E, Yang J (2011) Inferential ecosystem models, from network data to prediction. Ecol Appl 21(5):1523–1536
Clausen KK, Clausen P (2013) Earlier Arctic springs cause phenological mismatch in long-distance migrants. Oecologia 173(3):1101–1112
Cohen JM, Lajeunesse MJ, Rohr JR (2018) A global synthesis of animal phenological responses to climate change. Nat Clim Chang. https://doi.org/10.1038/s41558-018-0067-3
Crabbe RA, Dash J, Rodriguez-Galiano VF, Janous D, Pavelka M, Marek MV (2016) Extreme warm temperatures alter forest phenology and productivity in Europe. Sci Total Environ 563–564:486–495
Cushing DH (1969) The regularity of the spawning season of some fishes. ICES J Mar Sci 33(1):81–92
Descamps S, Ramírez F, Benjaminsen S, Anker-Nilssen T, Barrett RT, Burr Z, Christensen-Dalsgaard S, Erikstad K-E, Irons DB, Lorentsen S-H, Mallory ML, Robertson GJ, Reiertsen TK, Strøm H, Varpe Ø, Lavergne S (2019) Diverging phenological responses of Arctic seabirds to an earlier spring. Glob Change Biol 25(12):4081–4091
Doiron M, Gauthier G, Lévesque E (2015) Trophic mismatch and its effects on the growth of young in an Arctic herbivore. Glob Change Biol 21(12):4364–4376
Donnelly A, Caffarra A, O'Neill BF (2011) A review of climate-driven mismatches between interdependent phenophases in terrestrial and aquatic ecosystems. Int J Biometeorol 55(6):805–817
Dunn PO, Møller AP (2014) Changes in breeding phenology and population size of birds. J Anim Ecol 83(3):729–739
Dunn PO, Winkler DW, Whittingham LA, Hannon SJ, Robertson RJ (2011) A test of the mismatch hypothesis: how is timing of reproduction related to food abundance in an aerial insectivore? Ecology 92(2):450–461
Durant JM, Hjermann DØ, Anker-Nilssen T, Beaugrand G, Mysterud A, Pettorelli N, Stenseth NC (2005) Timing and abundance as key mechanisms affecting trophic interactions in variable environments. Ecol Lett 8(9):952–958
Duveneck MJ, Thompson JR (2017) Climate change imposes phenological trade-offs on forest net primary productivity. J Geophys Res Biogeosci 122(9):2298–2313
Edwards M, Richardson AJ (2004) Impact of climate change on marine pelagic phenology and trophic mismatch. Nature 430(7002):881
Elmore AJ, Guinn SM, Minsley BJ, Richardson AD (2012) Landscape controls on the timing of spring, autumn, and growing season length in mid-Atlantic forests. Glob Change Biol 18(2):656–674
Evans EW, Carlile NR, Innes MB, Pitigala N (2013) Warm springs reduce parasitism of the cereal leaf beetle through phenological mismatch. J Appl Entomol 137(5):383–391
Finley AO, Banerjee S, Gelfand AE (2015) SpBayes for large univariate and multivariate point-referenced spatio-temporal data models. J Stat Softw 63(1):1–28
Finley AO, Banerjee S, Gelfand AE (2013) SpBayes for large univariate and multivariate point-referenced spatio-temporal data models. ArXiv:1310.8192 [Stat]. http://arxiv.org/abs/1310.8192. Accessed 11 Dec 2023
Forrest JR (2016) Complex responses of insect phenology to climate change. Curr Opin Insect Sci 17:49–54
Forrest JRK, Thomson JD (2011) An examination of synchrony between insect emergence and flowering in Rocky Mountain meadows. Ecol Monogr 81(3):469–491
Freeman BG, Song Y, Feeley KJ, Zhu K (2021) Montane species track rising temperatures better in the tropics than in the temperate zone. Ecol Lett 24(8):1697–1708
Gaston AJ, Gilchrist HG, Mallory ML, Smith PA (2009) Changes in seasonal events, peak food availability, and consequent breeding adjustment in a marine bird: a case of progressive mismatching. The Condor 111(1):111–119
Hällfors MH, Antão LH, Itter M, Lehikoinen A, Lindholm T, Roslin T, Saastamoinen M (2020) Shifts in timing and duration of breeding for 73 boreal bird species over four decades. Proc Natl Acad Sci 117(31):18557–18565
Hipfner JM (2008) Matches and mismatches: ocean climate, prey phenology and breeding success in a zooplanktivorous seabird. Mar Ecol Prog Ser. https://doi.org/10.3354/meps07603
Huang B, Thorne PW, Banzon VF, Boyer T, Chepurin G, Lawrimore JH, Menne MJ, Smith TM, Vose RS, Zhang H-M (2017) Extended reconstructed sea surface temperature,

Version 5 (ERSSTv5): Upgrades, validations, and intercomparisons. J Clim 30(20):8179–8205
Hufkens K, Basler D, Milliman T, Melaas EK, Richardson AD (2018) An integrated phenology modelling framework in r. Methods Ecol Evol 9(5):1276–1285
Iler AM, Inouye DW, Høye TT, Miller-Rushing AJ, Burkle LA, Johnston EB (2013) Maintenance of temporal synchrony between syrphid flies and floral resources despite differential phenological responses to climate. Glob Change Biol 19(8):2348–2359
Jepsen JU, Kapari L, Hagen SB, Schott T, Vindstad OPL, Nilssen AC, Ims RA (2011) Rapid northwards expansion of a forest insect pest attributed to spring phenology matching with sub-Arctic birch. Glob Change Biol 17(6):2071–2083
Ji R, Jin M, Varpe Ø (2013) Sea ice phenology and timing of primary production pulses in the Arctic Ocean. Glob Change Biol 19(3):734–741
Jones T, Cresswell W (2010) The phenology mismatch hypothesis: are declines of migrant birds linked to uneven global climate change? J Anim Ecol 79(1):98–108
Jönsson AM, Appelberg G, Harding S, Bärring L (2009) Spatio-temporal impact of climate change on the activity and voltinism of the spruce bark beetle. Ips Typographus Glob Change Biol 15(2):486–499
Keenan TF, Richardson AD, Hufkens K (2020) On quantifying the apparent temperature sensitivity of plant phenology. New Phytol 225(2):1033–1040
Kharouba HM, Wolkovich EM (2020) Disconnects between ecological theory and data in phenological mismatch research. Nat Clim Chang. https://doi.org/10.1038/s41558-020-0752-x
Kharouba HM, Ehrlén J, Gelman A, Bolmgren K, Allen JM, Travers SE, Wolkovich EM (2018) Global shifts in the phenological synchrony of species interactions over recent decades. Proc Natl Acad Sci 115(20):5211–5216
Killmann W, Thong HL (1995) The periodicity of growth in tropical trees with special reference to dipterocarpaceae—a review. IAWA J 16(4):329–335
Kocarev L, Parlitz U (1995) General approach for chaotic synchronization with applications to communication. Phys Rev Lett 74(25):5028–5031
Koeller P, Fuentes-Yaco C, Platt T, Sathyendranath S, Richards A, Ouellet P, Orr D, Skúladóttir U, Wieland K, Savard L, Aschan M (2009) Basin-scale coherence in phenology of shrimps and phytoplankton in the North Atlantic Ocean. Science 324(5928):791–793
Kudo G, Ida TY (2013) Early onset of spring increases the phenological mismatch between plants and pollinators. Ecology 94(10):2311–2320
La Sorte FA, Graham CH (2020) Phenological synchronization of seasonal bird migration with vegetation greenness across dietary guilds. J Anim Ecol. https://doi.org/10.1111/1365-2656.13345
Liu Y, Reich PB, Li G, Sun S (2011) Shifting phenology and abundance under experimental warming alters trophic relationships and plant reproductive capacity. Ecology 92(6):1201–1207
MacKenzie CM, Johnston J, Miller-Rushing AJ, Sheehan W, Pinette R, Primack R (2019) Advancing leaf-out and flowering phenology is not matched by migratory bird arrivals recorded in hunting guide's journal in Aroostook county. Maine Northeast Naturalist 26(3):561–579
Masson-Delmotte V (2018) IPCC Special Report on Global Warming of 1.5 °C. WMO. https://www.ipcc.ch/sr15/. Accessed 6 Oct 2022
Mayor SJ, Guralnick RP, Tingley MW, Otegui J, Withey JC, Elmendorf SC, Andrew ME, Leyk S, Pearse IS, Schneider DC (2017) Increasing phenological asynchrony between spring green-up and arrival of migratory birds. Sci Rep 7(1):1–10
McKinney AM, CaraDonna PJ, Inouye DW, Barr B, Bertelsen CD, Waser NM (2012) Asynchronous changes in phenology of migrating Broad-tailed Hummingbirds and their early-season nectar resources. Ecology 93(9):1987–1993
McKinnon L, Picotin M, Bolduc E, Juillet C, Bêty J (2012) Timing of breeding, peak food availability, and effects of mismatch on chick growth in birds nesting in the High Arctic. Can J Zool 90(8):961–971
Medhaug I, Stolpe MB, Fischer EM, Knutti R (2017) Reconciling controversies about the 'global warming hiatus.' Nature. https://doi.org/10.1038/nature22315
Merkel B, Descamps S, Yoccoz NG, Danielsen J, Daunt F, Erikstad KE, Ezhov AV, Grémillet D, Gavrilo M, Lorentsen S-H, Reiertsen TK, Steen H, Systad GH, Þórarinsson ÞL, Wanless S, Strøm H (2019) Earlier colony arrival but no trend in hatching timing in two congeneric seabirds (Uria spp.) across the North Atlantic. Biol Let 15(10):20190634
Meza FJ, Silva D, Vigil H (2008) Climate change impacts on irrigated maize in Mediterranean climates: evaluation of double cropping as an emerging adaptation alternative. Agric Syst 98(1):21–30
Mjaaseth RR, Hagen SB, Yoccoz NG, Ims RA (2005) Phenology and abundance in relation to climatic variation in a sub-arctic insect herbivore–mountain birch system. Oecologia 145(1):53–65
Munch SB, Poynor V, Arriaza JL (2017) Circumventing structural uncertainty: a Bayesian perspective on nonlinear forecasting for ecology. Ecol Complex 32:134–143
Nakazawa T, Doi H (2012) A perspective on match/mismatch of phenology in community contexts. Oikos 121(4):489–495. https://doi.org/10.1111/j.1600-0706.2011.20171.x
Niclas J, Anders H, Per L (2007) Climate change and the optimal arrival of migratory birds. Proc Royal Soc B 274(1607):269–274
Nicola S, Roberto A, Diego R, von Jost H, Antonello P, Kathrin H, Ommo H, Aleksi L, Esa L, Kalle R, Maria R, Leonid S (2011) Climate warming, ecological mismatch at arrival and population decline in migratory birds. Proc Royal Soc b 278(1707):835–842
Ovaskainen O, Skorokhodova S, Yakovleva M, Sukhov A, Kutenkov A, Kutenkova N, Shcherbakov A, Meyke E, del Delgado MM (2013) Community-level phenological response to climate change. Proc Natl Acad Sci 110(33):13434–13439
Park DS, Breckheimer IK, Williams AC, Law E, Ellison AM, Davis CC (2018) Herbarium specimens reveal substantial and unexpected variation in phenological sensitivity

across the eastern United States. Philos Trans R Soc Lond B Biol Sci. https://doi.org/10.1098/rstb.2017.0394
Parmesan C, Yohe G (2003) A globally coherent fingerprint of climate change impacts across natural systems. Nature 421(6918):37
Paull SH, Johnson PTJ (2014) Experimental warming drives a seasonal shift in the timing of host-parasite dynamics with consequences for disease risk. Ecol Lett 17(4):445–453
Pearce-Higgins JW, Dennis P, Whittingham MJ, Yalden DW (2010) Impacts of climate on prey abundance account for fluctuations in a population of a northern wader at the southern edge of its range. Glob Change Biol 16(1):12–23
Petanidou T, Kallimanis AS, Sgardelis SP, Mazaris AD, Pantis JD, Waser NM (2014) Variable flowering phenology and pollinator use in a community suggest future phenological mismatch. Acta Oecologica 59:104–111
Plard F, Gaillard J-M, Coulson T, Hewison AJM, Delorme D, Warnant C, Bonenfant C (2014) Mismatch between birth date and vegetation phenology slows the demography of roe deer. PLoS Biol 12(4):e1001828
Post E, Forchhammer MC (2008) Climate change reduces reproductive success of an Arctic herbivore through trophic mismatch. Philos Trans Royal Soc B 363(1501):2367–2373
Post E, Pedersen C, Wilmers CC, Forchhammer MC (2008) Warming, plant phenology and the spatial dimension of trophic mismatch for large herbivores. Proc Royal Soc B 275(1646):2005–2013
PRISM Climate Group (2019) *PRISM Gridded Climate Data*. Oregon State University. https://prism.oregonstate.edu/
Qiu T, Song C, Clark JS, Seyednasrollah B, Rathnayaka N, Li J (2020) Understanding the continuous phenological development at daily time step with a Bayesian hierarchical space-time model: impacts of climate change and extreme weather events. Remote Sens Environ 247:111956
R Core Team. (2021). R: A language and environment for statistical computing. R Foundation for Statistical Computing, Vienna, Austria. https://www.r-project.org/. Accessed 11 Dec 2023
Rafferty NE, Ives AR (2011) Effects of experimental shifts in flowering phenology on plant–pollinator interactions. Ecol Lett 14(1):69–74
Rafferty NE, CaraDonna PJ, Bronstein JL (2015) Phenological shifts and the fate of mutualisms. Oikos (copenhagen, Denmark) 124(1):14–21
Ravignani A (2017) Interdisciplinary debate: agree on definitions of synchrony. Nature 545:158
Read JS, Jia X, Willard J, Appling AP, Zwart JA, Oliver SK, Kumar V (2019) Process-guided deep learning predictions of lake water temperature. Water Resour Res 55(11):9173–9190
Reed TE, Jenouvrier S, Visser ME (2013) Phenological mismatch strongly affects individual fitness but not population demography in a woodland passerine. J Anim Ecol 82(1):131–144
Remsberg EE, Deaver LE (2005) Interannual, solar cycle, and trend terms in middle atmospheric temperature time series from HALOE. J Geophys Res: Atmospheres. https://doi.org/10.1029/2004JD004905
Reneerkens J, Schmidt NM, Gilg O, Hansen J, Hansen LH, Moreau J, Piersma T (2016) Effects of food abundance and early clutch predation on reproductive timing in a high Arctic shorebird exposed to advancements in arthropod abundance. Ecol Evol 6(20):7375–7386
Renner SS, Zohner CM (2018) Climate change and phenological mismatch in trophic interactions among plants, insects, and vertebrates. Annu Rev Ecol Evol Syst 49(1):165–182
Richardson AD, Hufkens K, Milliman T, Aubrecht DM, Furze ME, Seyednasrollah B, Krassovski MB, Latimer JM, Nettles WR, Heiderman RR, Warren JM, Hanson PJ (2018) Ecosystem warming extends vegetation activity but heightens vulnerability to cold temperatures. Nature 560(7718):368
Riedmiller M, Braun H (1993) A direct adaptive method for faster backpropagation learning: the RPROP algorithm. IEEE Int Conf Neural Netw 1:586–591
Rockwell RF, Gormezano LJ, Koons DN (2011) Trophic matches and mismatches: can polar bears reduce the abundance of nesting snow geese in western Hudson Bay? Oikos 120(5):696–709
Rulkov NF, Sushchik MM, Tsimring LS, Abarbanel HDI (1995) Generalized synchronization of chaos in directionally coupled chaotic systems. Phys Rev E 51(2):980–994
Sanz JJ, Potti J, Moreno J, Merino S, Frías O (2003) Climate change and fitness components of a migratory bird breeding in the Mediterranean region. Glob Change Biol 9(3):461–472
Satterthwaite WH, Carlson SM, Allen-Moran SD, Vincenzi S, Bograd SJ, Wells BK (2014) Match-mismatch dynamics and the relationship between ocean-entry timing and relative ocean recoveries of Central Valley fall run Chinook salmon. Mar Ecol Prog Ser 511:237–248
Schiff SJ, So P, Chang T, Burke RE, Sauer T (1996) Detecting dynamical interdependence and generalized synchrony through mutual prediction in a neural ensemble. Phys Rev E 54(6):6708–6724
Seifert CA, Lobell DB (2015) Response of double cropping suitability to climate change in the United States. Environ Res Lett 10(2):024002
Senior VL, Evans LC, Leather SR, Oliver TH, Evans KL (2020) Phenological responses in a sycamore–aphid–parasitoid system and consequences for aphid population dynamics: a 20 year case study. Glob Change Biol 26(5):2814–2828
Seyednasrollah B, Swenson JJ, Domec J-C, Clark JS (2018) Leaf phenology paradox: why warming matters most where it is already warm. Remote Sens Environ 209:446–455
Shen M, Tang Y, Chen J, Zhu X, Zheng Y (2011) Influences of temperature and precipitation before the growing season on spring phenology in grasslands of the central and eastern Qinghai-Tibetan Plateau. Agric for Meteorol 151(12):1711–1722
Shipley JR, Twining CW, Taff CC, Vitousek MN, Flack A, Winkler DW (2020) Birds advancing lay dates with warming springs face greater risk of chick mortality.

Proc Natl Acad Sci. https://doi.org/10.1073/pnas.2009864117

Singer MC, Parmesan C (2010) Phenological asynchrony between herbivorous insects and their hosts: Signal of climate change or pre-existing adaptive strategy? Philos Trans Royal Soc B 365(1555):3161–3176

Song Y, Zajic CJ, Hwang T, Hakkenberg CR, Zhu K (2021) Widespread mismatch between phenology and climate in human-dominated landscapes. AGU Advances 2(4):e2021AV000431

Sugihara G, May RM (1990) Nonlinear forecasting as a way of distinguishing chaos from measurement error in time series. Nature 344(6268):734–741

Sugihara G, Grenfell BT, May RM, Tong H (1994) Nonlinear forecasting for the classification of natural time series. Philos Trans Royal Soc Lond. Ser a 348(1688):477–495

Takens F (1981) Detecting strange attractors in turbulence. In: Rand D, Young L-S (eds) Dynamical systems and turbulence, Warwick 1980. Springer, Berlin, pp 366–381

Thackeray SJ, Sparks TH, Frederiksen M, Burthe S, Bacon PJ, Bell JR, Botham MS, Brereton TM, Bright PW, Carvalho L, Clutton-Brock T, Dawson A, Edwards M, Elliott JM, Harrington R, Johns D, Jones ID, Jones JT, Leech DI, Wanless S (2010) Trophic level asynchrony in rates of phenological change for marine, freshwater and terrestrial environments. Glob Change Biol 16(12):3304–3313

Tikkanen O-P, Julkunen-Tiitto R (2003) Phenological variation as protection against defoliating insects: the case of Quercus robur and Operophtera brumata. Oecologia 136(2):244–251

Van Noordwijk AJ, McCleery RH, Perrins CM (1995) Selection for the timing of great tit breeding in relation to caterpillar growth and temperature. J Anim Ecol 64(4):451–458

Visser ME, Both C (2005) Shifts in phenology due to global climate change: the need for a yardstick. Proc Royal Soc B 272(1581):2561–2569

Visser ME, van Noordwijk AJ, Tinbergen JM, Lessells CM (1998) Warmer springs lead to mistimed reproduction in great tits (Parus major). Proc Royal Soc B 265(1408):1867–1870

Visser ME, te Marvelde L, Lof ME (2012) Adaptive phenological mismatches of birds and their food in a warming world. J Ornithol 153(1):75–84

Vitasse Y, Signarbieux C, Fu YH (2018) Global warming leads to more uniform spring phenology across elevations. Proc Natl Acad Sci 115(5):1004–1008

Wiesenfeldt M, Parlitz U, Lauterborn W (2001) Mixed state analysis of multivariate time series. Int J Bifurcation Chaos 11(08):2217–2226

Wu J, Serbin SP, Xu X, Albert LP, Chen M, Meng R, Saleska SR, Rogers A (2017) The phenology of leaf quality and its within-canopy variation is essential for accurate modeling of photosynthesis in tropical evergreen forests. Glob Change Biol 23(11):4814–4827

Yang LH, Rudolf VHW (2010) Phenology, ontogeny and the effects of climate change on the timing of species interactions. Ecol Lett 13(1):1–10

Yun K, Hsiao J, Jung M-P, Choi I-T, Glenn DM, Shim K-M, Kim S-H (2017) Can a multi-model ensemble improve phenology predictions for climate change studies? Ecol Model 362:54–64

Zhang X, Friedl MA, Schaaf CB (2006) Global vegetation phenology from Moderate Resolution Imaging Spectroradiometer (MODIS): Evaluation of global patterns and comparison with in situ measurements. J Geophys Res Biogeosci. https://doi.org/10.1029/2006JG000217

Zhang X, Liu L, Henebry GM (2019) Impacts of land cover and land use change on long-term trend of land surface phenology: a case study in agricultural ecosystems. Environ Res Lett 14(4):044020

Zimova M, Mills LS, Lukacs PM, Mitchell MS (2014) Snowshoe hares display limited phenotypic plasticity to mismatch in seasonal camouflage. Proc Royal Soc b. https://doi.org/10.1098/rspb.2014.0029

Zimova M, Mills LS, Nowak JJ (2016) High fitness costs of climate change-induced camouflage mismatch. Ecol Lett 19(3):299–307. https://doi.org/10.1111/ele.12568